Respiratory Airflow Estimation From Tracheal Breath Sound

By

Yee Leng Yap
daniely77@hotmail.com

A thesis submitted in partial fulfillment
Of the requirements for the degree

Master of Science in Electrical and Computer Engineering

University of Manitoba

July 2002

THE UNIVERSITY OF MANITOBA

FACULTY OF GRADUATE STUDIES

*****

MASTER'S THESIS/PRACTICUM FINAL REPORT

The undersigned certify that they have read the Master's Thesis/Practicum entitled:

Respiratory Airflow Estimation From Tracheal Breath Sound

submitted by

Yee Leng Yap

in partial fulfillment of the requirements for the degree of

M.SC.

The Thesis/Practicum Examining Committee certifies that the thesis/practicum (and oral examination if required) is:

(Approved or Not Approved)

☑ Thesis

☐ Practicum

Advisor: (Zahra Moussavi)

(Gabe Thomas)

(HANS PASTERKAMP)

Date: AUG 12/02

(forms\thereptm - 08/95)

THE UNIVERSITY OF MANITOBA

FACULTY OF GRADUATE STUDIES

*****

COPYRIGHT PERMISSION PAGE

RESPIRATORY AIRFLOW ESTIMATION FROM TRACHEAL BREATH SOUND

BY

YEE LENG YAP

A Thesis/Practicum submitted to the Faculty of Graduate Studies of The University of Manitoba in partial fulfillment of the requirements of the degree of

Master of Science

ABSTRACT

RESPIRATORY AIRFLOW ESTIMATION FROM TRACHEAL SOUND

Acoustical analysis of the respiratory sounds (Tracheal and Lung sounds) has been used to detect respiratory phases (Inspiration/Expiration) without airflow measurement [Moussavi et al., 2000]. This technique facilitates the estimation of airflow by locating the zero crossing of phase transitions from respiratory sounds. Using statistical analysis, previous studies have shown that there is a relationship between respiratory sounds and airflow. However, no attempt was made to estimate airflow and evaluate the error. Therefore, the purpose of this study was to determine the best model for airflow estimation by acoustical means. Based on some preliminary studies, an exponential model was used to estimate respiratory airflow from average power of tracheal sounds. The model needs only a few breath sounds recorded together with airflow measurements for calibration for each subject. The model parameters were derived from the breaths with known airflow and then applied to the rest of the breath sounds to estimate airflow. The model was tested by estimating airflow at various rates from tracheal sounds of ten healthy subjects. Because relationship between airflow and average power of tracheal sound was found to be different for inspiration and expiration [Mussell and Miyamoto, 1992, Mahagnah and Gavriely, 1994], the model parameters were derived for each phase separately. Estimated airflow was

compared to actual recorded airflow to determine the error. The results showed that the estimated airflow followed actual airflow well with an error of 4.84±2.39% of the target airflow. Apart from that, a new method to detect breath onsets from tracheal sound using variance fractal dimension was also investigated. Some results showed a delay of 40±9 *ms* between actual and detected breath onsets.

TABLE OF CONTENT

LIST OF FIGURES

Figures

ACKNOWLEDGEMENT

I wish to thank the Lord for giving me all the blessings in life. Also, I would like to dedicate this thesis to both my parents who love me unconditionally.

I am grateful to HsiaoYao Chen, for her constant encouragement and strong support throughout my studies here in Canada. I am really blessed to have known you and will always love you.

I would like to express my deepest gratitude to my advisor for this thesis project, Dr. Zahra Moussavi for her invaluable guidance and inspiration, especially her greatly appreciated patience during the course of my thesis. In the past two years, I was tremendously encouraged by her optimism about the project. Also, I would like to thank her for her critical reviews of the entire thesis and many constructive suggestions for improving my thesis writing. I would like to thank the Natural Science and Engineering Research Council of Canada (NSERC) for its support for this project.

I am deeply indebted to all the wonderful people stated above. May God bless you.

CHAPTER 1 - INTRODUCTION

I. Motivation

One of the important investigation areas of tracheal respiratory sounds concerns their relation with airflow. Variation in airflow rate is usually reflected by intensity change in tracheal and lung sounds [Charbonneau et al., 1987]. To date in clinical respiratory and/or swallowing assessments, airflow is usually measured by spirometry devices such as pneumotachograph, nasal cannulae connected to a pressure transducer (Figure 1.1) and/or heated thermistor anemometry. Airflow can also be measured by indirect means such as detection of chest and/or abdominal movements using respiratory inductance plethysmography (RIP), strain gauges, or magnetometers [Tarrant, et al., 1997]. The most reliable measurement of airflow is achieved by a mouth piece (Figure 1.1) or facemask connected to a pneumotachograph. However, they have the disadvantage of altering the breathing pattern of subjects or patients [Moussavi, et. al., 2000]. Furthermore, they are not applicable during swallowing and feeding assessments. The solution to circumvent this drawback is to use a nasal cannulae connected to a pressure transducer during the swallowing and feeding assessments. However, the use of a nasal cannulae is an inaccurate way of measuring flow signals because the air leaks around the nasal cannulae and in addition if the subject breathes through the mouth, the cannulae does not register flow. For these reasons, a combined use of a nasal cannulae connected to a pressure

transducer in addition to measurements of respiratory inductance to follow volume changes has been recommended as the best approach to assess respiratory patterns during swallowing assessments [Tarrant, et al., 1997]. However, the application of these techniques remains a challenge when children with neurological impairments are involved because they normally do not cooperate during signals recording [Moussavi et al., 2000]. Hence, the motivation of this thesis was to investigate the possibility of replacing the cumbersome airflow measurement techniques by estimating it through respiratory sounds, i.e., tracheal breath sounds.

The tracheal breath sounds were chosen because they are higher in intensity, observable over a wider frequency range and easier to capture than the sounds from the chest wall (lung sounds) [Pasterkamp et al., 1997; Gavriely et al., 1995]. Furthermore, there are stronger correlations between airflow and tracheal sound intensities and/or their mean frequencies [Charbonneau, et al., 1987]. If an acceptable mathematical model materializes, it will greatly simplify the clinical respiratory assessments with less intrusion and also enhance the studies of clinical relevance between the two variables.

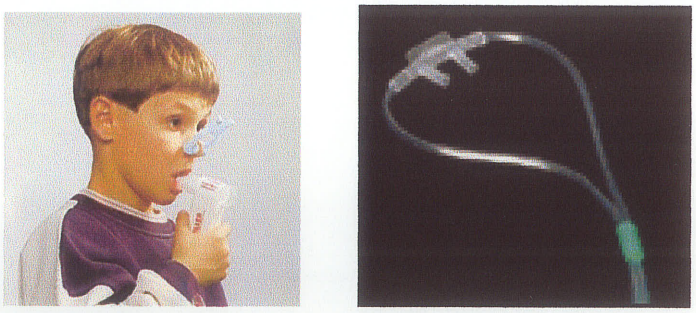

Figure 1.1. Spirometry devices: pneumotachograph (left) and nasal cannulae (right).

II. Background

Respiration is a process by which an organism exchanges gases with its environment. During the course of airlfow exchange, respiratory sounds are generated. The generation of tracheal sounds is primarily related to turbulence of air in the upper airways, including pharynx, glottis and subglottis region (The lower part of the larynx; the area from just below the vocal cords down to the top of the trachea.) (Figure 1.2). Flow turbulence and jet formation at the glottis cause pressure fluctuations within the airway lumen. Sound pressure waves within the airway gas and airway wall motion are likely contributing to the vibrations that reach the neck surface and are recorded as tracheal sounds. Because of the proximity of the sound source and the pickup area at the neck and the lack of interposition of lung tissue, tracheal sounds are universally regarded as wide bandwidth respiratory sounds [Pasterkamp et al., 1997].

The interest of studying respiratory sounds commenced since Laennec's paper [Leännec, 1819] on relationship between human pulmonary diseases and respiratory auscultation was published in 1935. The diagnosis of these diseases is facilitated by pulmonary auscultation using a stethoscope, which was invented in 1821 by the French Phycisian, Laennec. Until a few decades ago, physicians were relying on their hearing of the patients' respiratory sounds to detect any pathological symptoms. However, it is a subjective perception by individual physician. Moreover, the stethoscope has a frequency response that attenuates frequency components above 120 *Hz*, and the human ear is not very sensitive to frequencies lower than 120 *Hz* [Abella et al., 1992]. Over the recent

years, computer technology has been increased markedly in the field of respiratory acoustics and breath sound analysis. This technology has drawn much attention because of its diagnostic features. For example measurement of sound intensity and its spectral shape have already been used to provide a noninvasive indication of airflow in sleep studies [Cummiskey et al., 1982] and as a basis of apnea monitoring [Backerman et al., 1985]. There is also evidence that such measurements may be of value in diagnosing and monitoring tracheal obstruction, and it should be possible to use tracheal sound analysis as a mean of indicating the occurrence of structural and dynamic changes in the upper airway [Plante et al., 1998]. With the availability of high-tech acoustical devices such as air coupled microphones and contact accelerometers that are more sensitive and specific for respiratory assessment, and novel signal processing methods [Priestley, 1981; Gasquet et al., 1990; Earis et al., 2000; Charbonneau et al., 2000, Vannuccini et al., 2000], we are now embarking on the next generation of pulmonary assessment techniques based on acoustical means.

In any pulmonary assessment, respiratory airflows are usually measured simultaneously with breath sounds for analysis as the two signals contain different but complimentary information that is helpful for understanding the underlying pathophysiology in the pulmonary system. Apart from that, knowledge of respiratory sounds along with airflow posts the advantage of understanding the mechanisms involved during the generation (origin) of respiratory sounds [Bullar, 1884], which up to present has remained a challenge despite the multitude of investigations [Forgacs et al., 1969; Fahr et al., 1927; Olson et al., 1985; Gavriely et al.,1981].

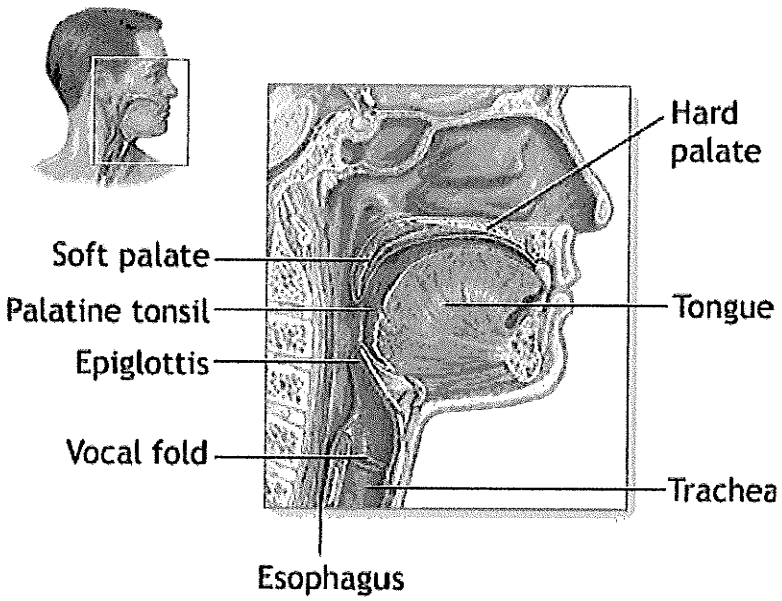

Figure 1.2. Anatomy of the respiratory tract.

Therefore, in clinical respiratory assessments, it is necessary to have airflow information along with respiratory breath sounds. Conventionally, spirometry devices such as pneumotachograph, nasal cannulae with pressure transducer, heated thermistor anemometry, etc., are used for assessing flow rate. However, these methods have the disadvantage of altering the breathing pattern of the subject. In addition, although the application of a nasal cannulae seems like a minor intrusion, it can cause significant agitation when conducting respiratory and swallowing assessment in children with neurological impairment [Moussavi et al., 2000]. Furthermore, applying these devices to young patients, which require full patients' co-operation is a challenging task for physicians and researchers. The situation is worsen for patients with physical deformities and poor posture control [Moussavi et al., 2000]. Hence we sought to develop an alternative, non-invasive method to estimate airflow by acoustical means.

Recently, a non-invasive acoustical phase detection algorithm using lung and tracheal sounds has been developed [Moussavi et al., 2000]. In that method, the respiratory phases together with breath onsets (inspiration→expiration / expiration→inspiration) were detected acoustically with 100% accuracy. This study aimed to proceed further by estimating airflow acoustically in order to fully eliminate the need of airflow measurements in clinical assessments.

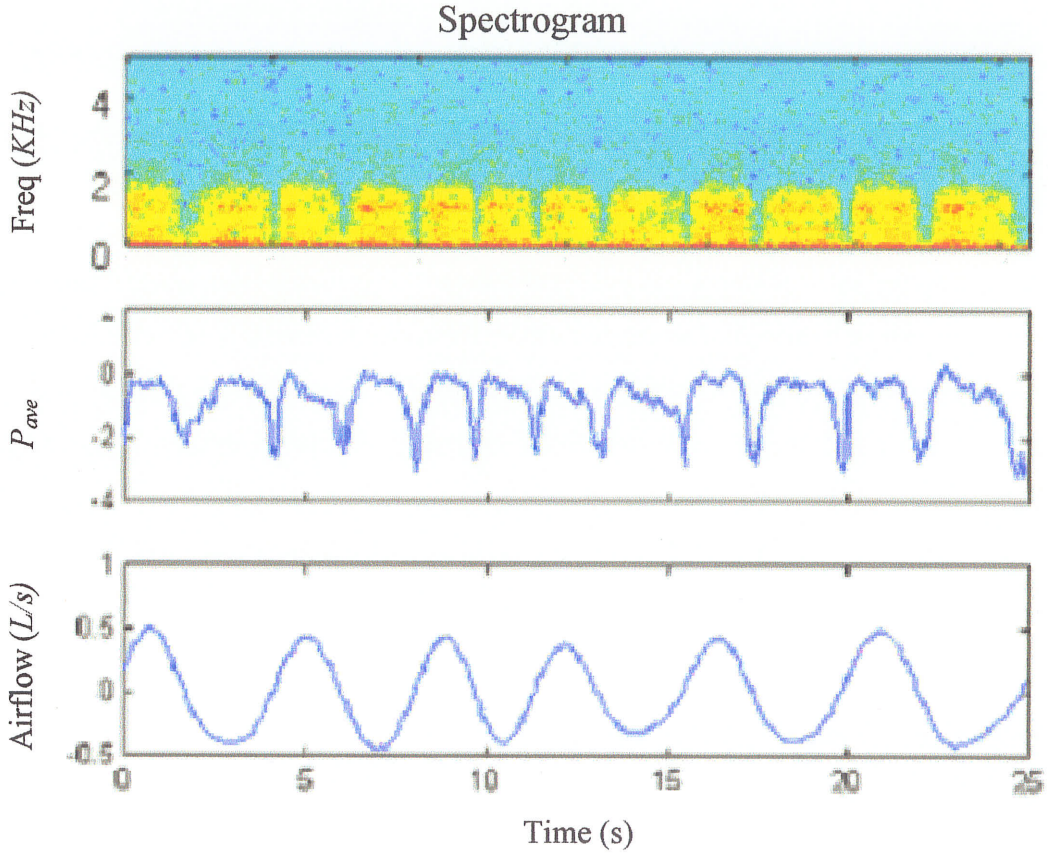

Figure 1.3. Three typical plots (from top to bottom) of spectrogram, P_{ave} and airflow

Figure 1.3 shows the spectrogram, average power of tracheal sound (P_{ave}) and its corresponding airflow of a typical breath sound. As it can be observed, there is a relationship between airflow and average power of tracheal sounds. During a peak flow-

rate of both inspiration and expiration, the average power of the tracheal sound approaches local maximum at the neighboring location. To achieve the goal of estimating airflow acoustically, several mathematical models that can represent the relationship between airflow and average power of the tracheal sounds was investigated, and the best model was used to estimate airflow. Figure 1.4 shows a typical tracheal signal recording for inspiration, expiration followed by four seconds of breath-hold. The breath-hold segments represent the environmental conditions (background noise), which is not directly induced by breathing during respiratory sounds recording, and should be subtracted from breath segments to avoid bias.

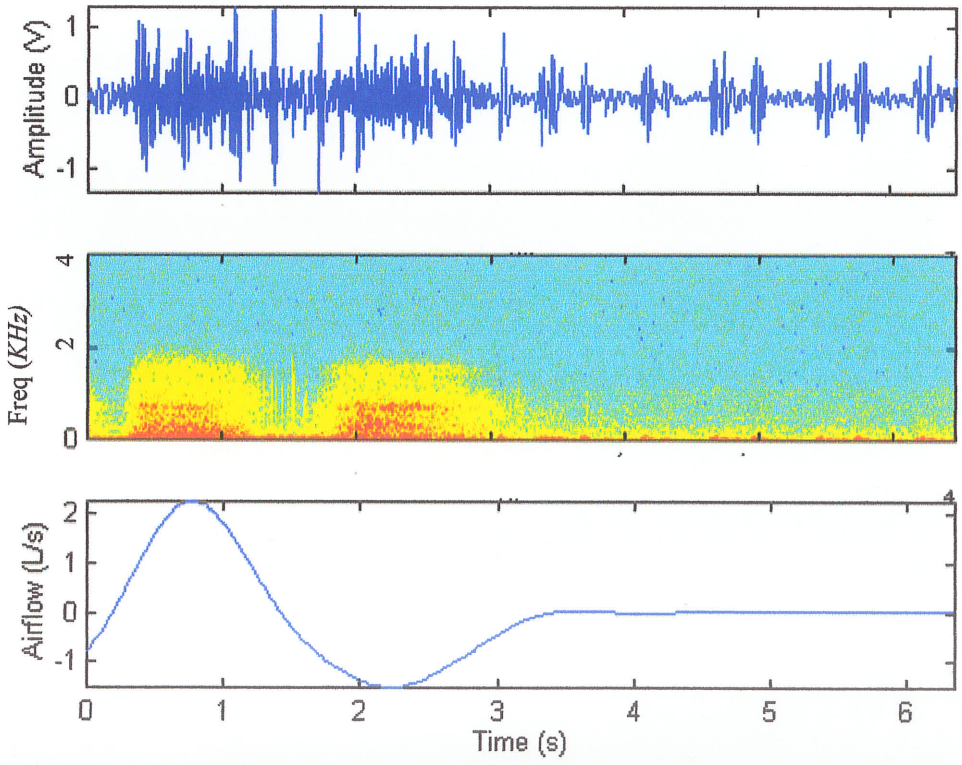

Figure 1.4. A typical tracheal sound signal, including inspiration, expiration and four seconds of breath-hold at the end of a recording (top figure) and the corresponding airflow signal (bottom figure).

Using both tracheal and lung sounds, a recent study has detected the onsets of breath acoustically [Moussavi at el., 2000]. In this study, however, a new method to detect breath onsets from tracheal sound using variance fractal dimension D_σ was also investigated.

In summary, the objectives of this study were to:

1. investigate the best model that can represent the relationship between tracheal sound's average power and airflow,
2. use this best model to estimate airflow,
3. investigate a new method for detection of breath onsets.

III. Thesis Outlines

Chapter 1 – The objective of this chapter is to present the motivations and background information for this thesis. It overviews the respiratory system and sounds mechanism briefly and defines the research goal.

Chapter 2 – This chapter gives an overlook of past research done on tracheal signals, which encompasses the studies of tracheal signal characteristics as well as its relationship with airflow. Each proposed model has a coarse expository of its methodology along with error analysis if one was available.

Chapter 3 – This chapter presents the signal processing techniques and mathematical models used in this study. Topics include the derivation of average power (P_{ave}) from raw data of tracheal sounds, investigation of different frequency bands from which P_{ave} can be computed, error definition for target airflow estimation, different model equations, scaling factor for adjusting the model, the effect of different lower limit of fitting region of the breath sound and flow on estimation accuracy, the effect of deriving model coefficients from different base regions and a new method for breath onsets detection using a variance fractal dimension algorithm.

Chapter 4 – This chapter presents the results of determining the optimum parameters for airflow estimation, i.e., optimum lower limit for fitting region of airflow and P_{ave}, optimum frequency band from which P_{ave} was computed and base region to derive model

coefficients. Later, using the optimum parameters, results of airflow estimation are presented together with the error analysis across 10 subjects. The result of breath onset detection and the method's accuracy is also presented.

Chapter 5 -- This chapter gives a discussion on the results of the current study and recommendation for future research.

CHAPTER 2 - LITERATURES REVIEW

I. Review of Relevant Research Papers

The study of respiratory sounds using a computer has a considerable history, which spans a time of rapidly evolving technology and changing perception of analogue and digital signal processing. Much of the knowledge gained in the recent years has resulted from the use of a wide variety of data acquisition and signal processing techniques in various areas of respiratory research [Priestley, 1981; Gasquet et al., 1990; Earis et al., 2000; Charbonneau et al., 2000; Vannuccini et al., 2000]. Based on research publications, studies concerning upper airway sounds (tracheal sounds, cough and stridor) were found to make up 63% of the total world publications referring to upper and lower respiratory sounds over ten years from January 1986 to January 1996. The study of wheeze produced 26% of the total, and the study of a variety of other respiratory sounds (i.e., hoarseness of voice) made up the remaining percentage [Earis et al., 2000]. This shows the increasing interest in the study of upper airway sounds, especially for its clinical implications. Below are relevant papers discussing tracheal sound characteristics and their relationship with respiratory airflow.

Early research on the relationship between tracheal sound and airflow commenced when experiments showed that increasing the airflow caused parallel upward shifts of the spectral curve with no changes in the general pattern of the tracheal sound spectrum [Leblanc et. al., 1970, Charbonneau et. al., 1987] or in the frequencies of resonances [Pasterkamp et. al., 1997]. Other recent studies revealed that increasing airflow modified both intensity and the frequency distribution of the tracheal sound spectrum [Ploysongsang et al., 1982; Lessard et al., 1986; Kraman et al., 1998]. The relationship between flow and breath sound depends on many factors including upper airways configuration and, especially the chest volume of the subject. However, for every subject the mean amplitude and the mean power frequency are increasing as a function of flow [Charbonneau et al., 1987; Soufflet et al., 1990]. For this reason, researchers investigated various methods to relate these two signals [Forgacs et al., 1978; Mussell et al., 1990; Mussell et al., 1992; Soufflet et al., 1990; Gavriely et al., 1996] and some researchers used the relationship to estimate flow from breath sounds.

Tracheal sound has been characterized as a broad spectrum signal, covering a wide frequency range from less than 100 *Hz* to more than 1500 *Hz* with a sharp drop in power above a cutoff frequency of approximately 800 *Hz* [Gavriely et al., 1981]. It has also been shown that the spectrum of the tracheal sound exhibits peaks and troughs that are related to airways dimensions and are dependent on gas density [Pasterkamp et al., 1997]. Sanchez and Pasterkamp [Sanchez et al., 1993], who investigated the relationship between the cutoff frequency of the tracheal sound power and body height, found that children with shorter tracheal lengths have a higher cutoff frequency than adults. In spite

of the complex dependency of tracheal sound signals on various parameters (height, airways dimension, gas density, etc), researchers were able to investigate the relationship between the airflow and tracheal sounds by considering subjects in the same category, having similar height and morphological structures.

The relationship between tracheal sound's amplitude and/or power with airflow has been studied by several researchers. Olson [Olson et al., 1984, Olson et al., 1985] discussed the relationship between tracheal sounds and airflow by measuring flow-induced noise (jet noise) in a model of the trachea with an artificial glottis and concluded a third order relationship between the two variables. Using statistical analysis, Shykhoff and her co-workers [Shykoff et al., 1988] demonstrated a quadratic relationship between the breath sound and airflow. However, in their study it was found that the envelopes of the recorded tracheal sounds had consistent fluctuations that limited their accuracy for airflow estimation. For that reason, they did not estimate airflow.

Lessard [Lessard et al., 1986] studied the relationship between a constant flow rate and the frequency spectrum of respiratory sounds when measured at the trachea. Respiratory sounds at six flow rates were measured with an electronic stethoscope placed at the inferior position of the circoid cartilage. Their results showed that the mean frequency of the power spectrum increased linearly with an increase in airflow but remained about the same when the flow rate was above 0.75 *L/s*. In addition, the expiratory spectra had higher mean frequency than inspiratory spectra.

Charbonneau [Charbonneau et al., 1987] used a another equation to relate airflow (F) with breath sound amplitude (BSA) in *Watts* and mean power frequency ($\overline{f}$). However, by breath sound amplitude they meant the area under the spectral curve of tracheal sound minus background noise. The model was summarized as

$$\overline{BSA} = AF/(k\overline{f} - F),$$

where F is flow in *L/s*, $\overline{BSA}$ is mean of BSA from the breath sounds recorded at four different locations, $\overline{f}$ is mean power frequency in *Hz*, A and k are constants. Further inspection of this model reveals a nonlinear relationship. According to their model, if $k\overline{f} >> F$, the tracheal sound spectral amplitude becomes linearly dependent on airflow. But as flow increases relative to $k\overline{f}$, the relationship becomes nonlinear with higher dependency on $\overline{BSA}$. They demonstrated that when increasing flow from 0.25 *L/s* to 0.5 *L/s*, $\overline{BSA}$ and flow had a power relationship ($BSA = kF^{\alpha}$) with α to be approximately 1.6, whereas increasing flow from 0.4 *L/s* to 0.8 *L/s*, α was about 2.6.

On the other hand, Soufflet and his co-workers [Soufflet et al., 1990] used eight different methods to estimate flow acoustically, using spectral parameters. A common way to characterize a frequency spectrum is to divide it into parts, such that each part represents the same amount of energy. The fractions can be halves (median), quarters (quartiles) or any percentage (percentiles) of the total spectrum energy. For instance the median frequency (f_{50}) is the frequency dividing the power spectrum into two parts of equal energy. Mean amplitude of spectrum can also be used as a signature for each

spectrum. Making use of these signal characteristics, Soufflet [Soufflet et al., 1990] estimated airflow from tracheal sounds with eight methods divided into two groups of four. For the first group of experiments, they assumed that a relationship existed between the flow and various tracheal signal parameters (mean amplitude of sound (in time-domain), mean amplitude of spectrum, mean frequency of spectrum and the product of mean amplitude and mean frequency). For each parameter, a specific reference curve was derived for each subject, representing the variation of the parameter versus flow. For the second group of experiments, each subject performed three recordings at low, tidal and high flow rate. A clustering algorithm was performed to build a set of cluster with the spectra as homogeneous as possible. The top of the cluster tree covered the entire spectra set of the data. Clusters with more than 20 spectra were divided into two clusters according to the homogeneity of spectra. This process was stopped when 40 clusters were obtained at the bottom of the tree. Each cluster was treated as a class associated to a corresponding airflow level. This relationship between spectra classes and airflow was used to evaluate airflow. Eight methods gave an error of about 14% except one method that resulted in 31% error.

In contrast to all researches who assumed that a relationship exists between tracheal sound and airflow, Mussel and his co-workers [Mussell et al., 1990, Mussell et al., 1992] claimed that tracheal and lung respiratory sounds are independent of flow over the range of 1.6-2.6 *L/s*. This result may look to stand in contrast to all other observations that respiratory sounds and airflow varies in certain pattern. However, the majority of other researchers investigated flow rates ranges which were below 1.6 *L/s*. Furthermore, it is in

agreement with Lessard and Wong [Lessard et al., 1986] who claimed that the mean power frequency remains the same for flow rates above 0.75 *L/s*.

More recently, Gavriely and his co-workers [Gavriely et al., 1996] investigated a power relationship between tracheal sound amplitude (BSA) and flow, as described by the following equation,

$$BSA = kF^{\alpha}, \qquad (2.1)$$

where F is airflow in *L/s*, α and k are constants. By amplitude, they actually meant the sound average power, which was calculated over the frequency band of 100-1000 *Hz* for the lung sounds and 100-2400 *Hz* for tracheal sound. The model was tested on the data recorded from six normal men. In their studies, lung and tracheal sounds were proven to exhibit the power relationship as stated above. However, they reported neither the mean square error of such a linear relationship between Log(*BSA*) and Log(*F*), nor the correlation coefficient between the two variables. Furthermore, they did not attempt to implement their model to estimate airflow. The overall mean±SD (standard deviation) value of the power coefficient (α) was determined to be 1.66±0.35. They also observed that lung sound power during inspiration was comparatively larger than that during expiration, whereas tracheal sound power was independent of respiratory phases, which was a common observation found in many studies.

Recently, effort has been concerted on several possible relationships between airflow and tracheal average power over different frequency bands. The outcomes consistently showed that the relationship between airflow and tracheal sounds can be best represented by an exponential model for tracheal sounds [Yap and Moussavi, 2002]. Therefore in this

study, three models (linear ($P_{ave}=kF$), power ($P_{ave}=kF^{\alpha}$) and exponential ($P_{ave}=ke^{F\alpha}$) relationship model) were investigated in more depth and the best model was used to estimate airflow. The error analysis was later computed by comparing the estimated and actual recorded airflow.

As it was mentioned in the previous chapter, a recent study has used tracheal and chest sounds to detect respiratory phases as well as breath onsets independent of airflow [Moussavi et al., 2000]. In current study however, variance fractal dimension algorithm of the tracheal sound signal was implemented as another approach to detect the breath onsets.

Fractal dimension is a measure of complexity in a data set, either two or three dimensional images or one-dimensional signals. It is used to analyze chaotic and non-chaotic signal in a wide range of scientific research, particularly in image compression, segmentation and in genetic maps [Faloutsos and Kamel, 1994; Faloutsos and Gaede, 1996; Traina at al., 2000]. Fractal dimension quantifies the complexity of an object which is obscure to human eyes. Variance fractal dimension D_σ (Equation 2.2) is one of the ways to calculate fractal dimension [Kinsner, 1995; Kinsner and Grieder, 1995].

$$D_\sigma = D_E - 1 + H , \qquad (2.2)$$

where D_E is the embedding dimension, which is the dimension of the embedding space (i.e., for a curve $D_E = 1$, a plane $D_E = 2$, and for space $D_E = 3$) and ,

$$H = \lim_{\Delta t \to 0} \frac{\log \mathrm{var}(\Delta S)_{\Delta t}}{2\log(\Delta t)} \quad , \qquad (2.3)$$

where S is the sound data samples and therefore ΔS is the variation of tracheal sound signal between two points as defined below:

$\Delta t = | t_2 - t_1 |$,

$(\Delta S)_{\Delta t} = S(t_2) - S(t_1)$,

Generally, fractal dimension can be obtained by taking the limit of the quotient of the log change of the object size and the log change of the measurement scale, as the measurement scale approaches zero (Equation 2.3). In deriving variance fractal dimension for one-dimensional data, the sampled signal is the "object", variance (σ) of the sampled signal is the "object size", while the time interval between the samples used to calculate the variance, is the "measurement scale" (Δt_k). One property of fractal dimensions is that they are independent of power content in the signal. This indicates that all signals, both with high or low amplitude, would produce the same magnitude of fractal dimension as long as they are composed of the same frequency components. In other words, fractal dimension calculates the complexity of a signal and is immune to signal amplitude.

In this study, a chaotic feature during the short period of time between the phases (inspiration→expiration or expiration→inspiration) was postulated. Therefore, we hypothesized that variance fractal dimension of respiratory sound peaks at the breath

onsets and this might lead to a better approach in the automated detection of the breath onsets by acoustical means.

CHAPTER 3 - METHODS AND PROCEDURES

I. Data

All data used in this research, were collected at the Respiratory Acoustics Laboratory, Children Hospital Winnipeg [Moussavi et al., 2000]. Data from ten subjects who had breathed at different flow rates were chosen in this study. Tracheal and lung respiratory sounds were recorded simultaneously with airflow. In this research, however, only the tracheal sounds were used. The sound signals were amplified, band-pass filtered (50-2500 *Hz*) and digitized at a 10240 *Hz* sampling rate. With a nose clip in place, airflow was measured with a mouthpiece attached to a calibrated pneumotachograph (Fleisch no. 3) and was digitized simultaneously with breath sounds at the same sampling rate. However, it was later decimated to 320 *Hz*. In all subjects, breath sounds were recorded at "low (0-0.4 *L/s*)", "medium (0.4-0.8 *L/s*)" and "high (0.8-1.4 *L/s*)" flow rates. Subjects watched their airflow signal on the computer screen and were encouraged to breathe at the target flow rate consistently for a minimum of five complete breaths at each level followed by a five-second breath-hold as the reference for background noise. The details of the experiments can be found in [Moussavi et al., 2000].

Inspiratory and expiratory sounds were extracted from the tracheal sound using the corresponded airflow signal. The goal was to investigate the relationship of the tracheal sound in each phase with airflow separately, since it is commonly known that inspiratory and expiratory phases exhibit distinct spectral characteristics [Mussell et al., 1992].

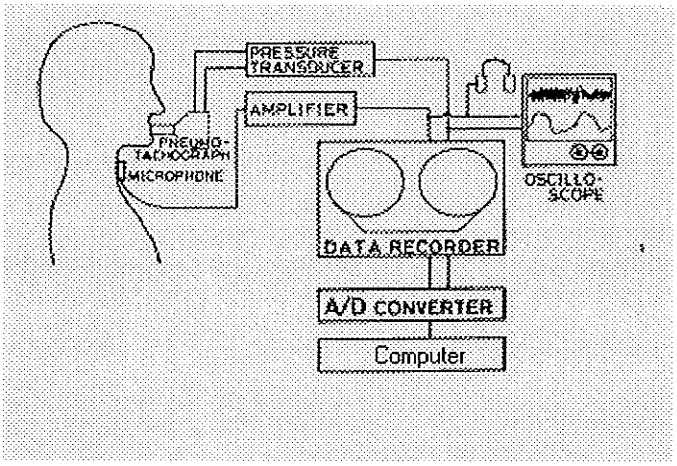

Figure 3.1. Recording system apparatus.

II. Signal Processing

i. Computing Average Power of Tracheal Sound

The tracheal sound signals were divided into 1024-sample segments (100 *ms*), with 50% overlap between successive segments. The power spectrum of each segment was calculated using FFT and applying a Hanning window to each segment. Initially, the average spectral power was calculated from the frequency band 100-800 *Hz* because spectral characteristics of tracheal sound are known to experience sharp attenuation above cutoff frequency of approximately 800 *Hz* [Gavriely et al., 1981]. However, a test

was run to find the best frequency band for calculating P_{ave}, which resulted in the best airflow estimation with the least error.

ii. Choosing an Appropriate Model

The first and foremost issue was to study the relationship between P_{ave} and airflow such that an appropriate model (linear, power or exponential model) could be selected to estimate respiratory airflow. The following three models were studied for a linear relationship.

1) $P_{ave} \propto F \rightarrow$ Linear relationship model,

2) $\text{Log}_{10}(P_{ave}) \propto \text{Log}_{10}(F) \rightarrow$ Power relationship model,

3) $\text{Log}_{10}(P_{ave}) \propto F \rightarrow$ Exponential relationship model,

where F is the calibrated amplitude of the airflow signal. The model, which achieved the least mean square error in regression line was chosen as the best model to estimate airflow from tracheal sound. In this part, P_{ave} was calculated over the frequency band 100 – 800 *Hz* and it was averaged between the subjects for each flow rate, from 0 to 1.4 *L/s* with a step size of 0.05 *L/s*.

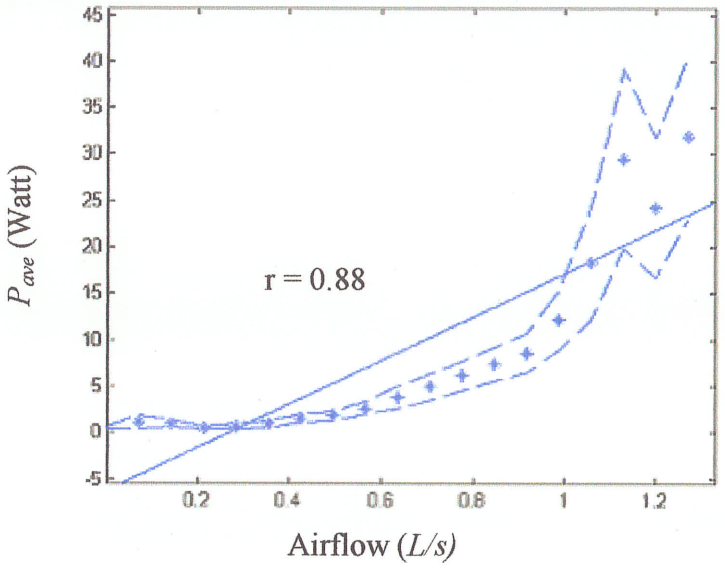
45
40
35
30
25
20
15
10
5
0
-5
0.2
0.4
0.6
0.8
1
1.2
r = 0.88
P_{ave} (Watt)
Airflow (*L/s*)

(a)

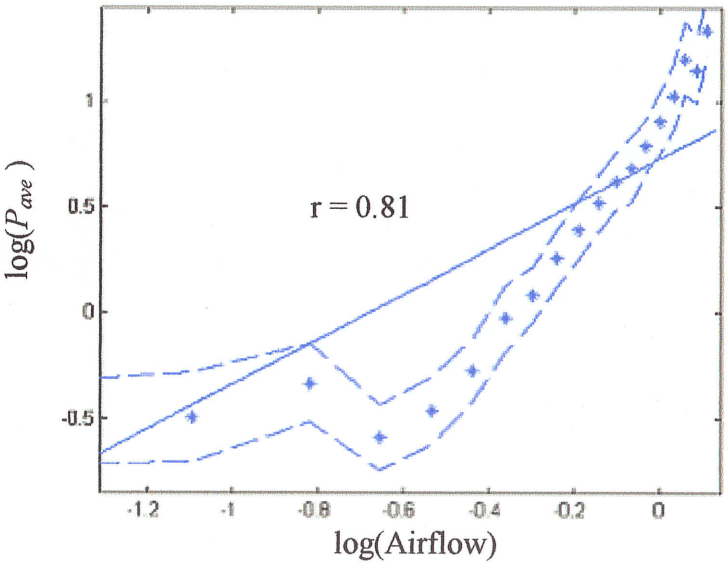
1
0.5
0
-0.5
-1.2
-1
-0.8
-0.6
-0.4
-0.2
0
r = 0.81
log(P_{ave})
log(Airflow)

(b)

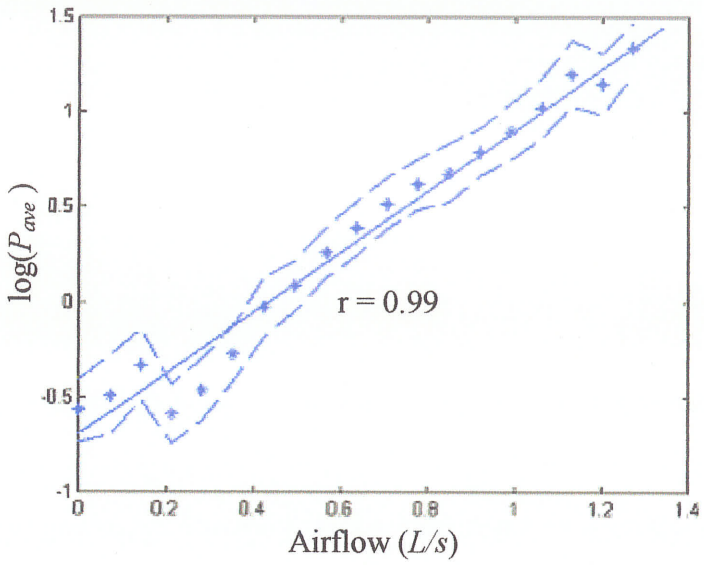

(c)

Figure 3.2. Relationship between a) P_{ave} and airflow, b) log(P_{ave}) and log(airflow), c) log(P_{ave}) and airflow. The star (*) points are the averaged P_{ave}) between the subjects while the dashed(--) lines show the standard error. The solid line is the regression line between the two variables in each plot and r is the correlation coefficient.

As can be seen in Figure 3.2 (a)—(c), the exponential model had the highest correlation coefficient (r =0.99); hence the linear fit error between $\log_{10}(P_{ave})$ and airflow was the least. Therefore, it was chosen as the best model for estimating airflow from average power of tracheal sound. Initially, the model was chosen as:

$$F_{est} = C_1 \log(P_{ave}) + C_2, \qquad (3.1)$$

where F_{est} is the estimated flow and C_1 and C_2 are the model coefficients.

III. Error Definition

The estimation error was defined as

$$Error = \left| \frac{mean(F_{est}) - mean(F_{actual})}{mean(F_{actual})} \right|, \qquad (3.2)$$

where the mean( ) was calculated from the average of the upper 15% of the airflow signal.

IV. Deriving the Model Coefficients

Five breaths of inspiration (expiration) at each of low, medium and high flow-rate were selected with their corresponding tracheal signals. As a reference to choosing only single flow rate region, a mixed base region (consisting two breaths from each level of flow rates) was also selected. The model coefficients were derived by fitting a line to the $\log_{10}(P_{ave})$ and airflow that minimized the least mean square error. The region (chosen either from low, medium or high flow rate), where these coefficients were derived from, was defined as the base region and then the model equation was used to estimate the remaining airflow signal samples from the tracheal average power measurements.

V. Modifying the Model Equation with a Scaling Factor

A pilot study of this research showed that when the coefficients of the model in Equation 3.1 were derived from a certain flow rate and then used to estimate other flow rates, the estimated flow was consistently underestimated or overestimated. This is shown in Figure 3.3. In order to remedy this problem, Equation 3.1 was modified by

incorporating a scaling factor to justify for different target flows as shown in Equation 3.3. We found that the best scaling factor is in the form of a ratio between the average power of the segment that its associated flow is being estimated and the average power of the base segments that were used to derive the coefficients.

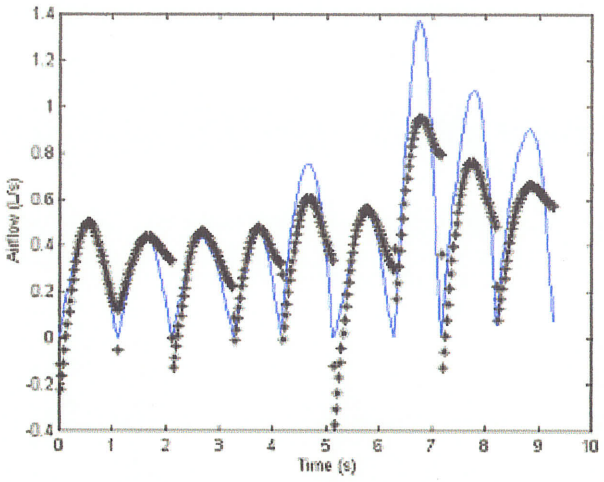

Figure 3.3. Actual (solid line) and estimated airflow (stars).

Equation 3.1 with the scaling factor can be written as:

$$F_{est} = (C_1 \log(P_{ave}) + C_2)(\frac{P_{segment}}{P_{base}})^k, \qquad (3.3)$$

where k is a constant and is determined from two known breath sounds with airflow that is assumed to be available for calibration. For example, if the model coefficients C_1 and C_2 are derived from medium target flow, k consisting of k_{low} *and* k_{high}, is determined by minimizing the error using two known breaths at low and high known flow rates, respectively. Note that the scaling factor in Equation 3.3 becomes 1 for the base segments.

VI. Selecting the Base Region

Bacause the subjects may breathe at different flow rates, the model should be robust enough to estimate airflow at any rates. Therefore, it is important what flow rate is chosen as the base to derive the model coefficients. In order to find which base region results in the least error, three different bases (low, medium and high) for deriving the model coefficients were investigated.

VII. Optimizing Target Airflow Estimation

As it was mentioned earlier, when deriving the model coefficients, the entire airflow from base segments was fitted to their corresponding P_{ave}. However, since the main interest was to estimate the target flow rate region accurately, P_{ave} can be fitted to the airflow only when it exceeded the lower limit of target flow rate region. Doing this proved to achieve better airflow estimation result. By changing the lower limit of airflow from 10% to 90% (equivalently upper 90% to 10%), the effect of fitting P_{ave} to airflow was investigated (Figure 3.4).

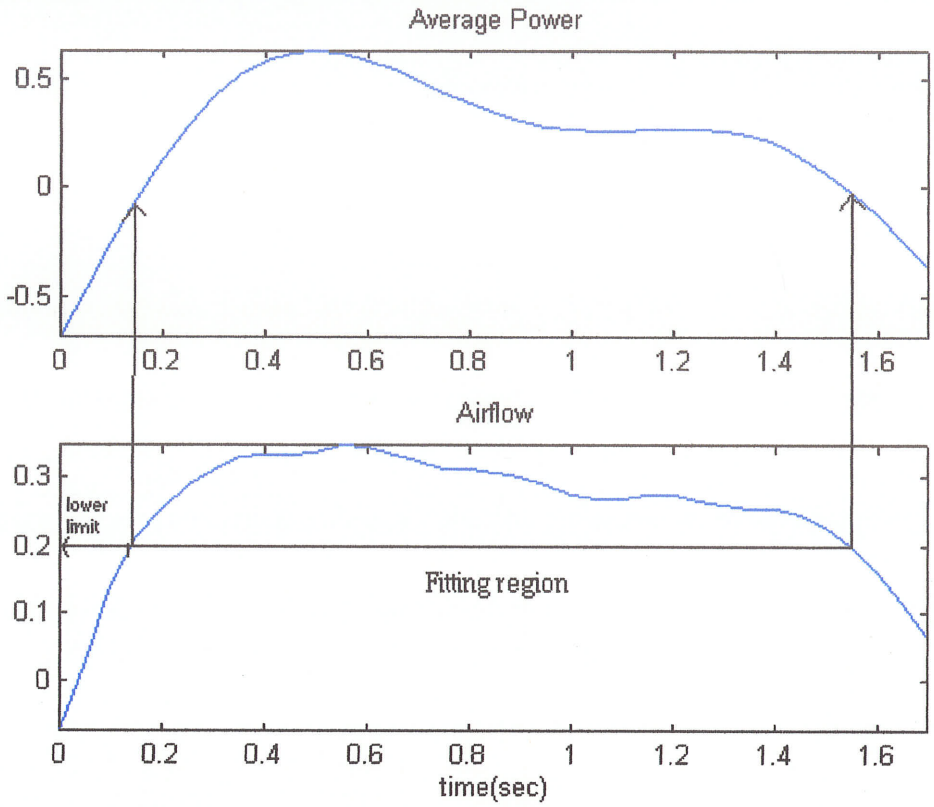

Figure 3.4. Optimization of target airflow estimation by having a lower limit for fitting region.

VIII. Frequency Band for Calculating P_{ave}

Bacause the spectral characteristics of tracheal sounds vary at different airflow rates, we tried to determine a frequency band where P_{ave} had the highest correlation with airflow. In order to investigate this issue, P_{ave} was calculated from nine different frequency bands: 100 – 300 *Hz*, 300 – 600 *Hz*, 600 - 1200 *Hz*, 100 – 600 *Hz*, 100 – 1200 *Hz*, 300 – 1200 *Hz*, 100 – 800 *Hz*, 100 – 450 *Hz*, 150 – 450 *Hz*. The frequency band that achieved the minimum error of flow estimation was chosen as the best frequency band.

IX. Summary of Airflow Estimation

Figure 3.5 shows the summary for airflow estimation in the form of a flow chart. The same process was applied to each subject so that each subject's signal had its own model coefficients, and scaling factors, which were used to estimate the remaining airflow from P_{ave}.

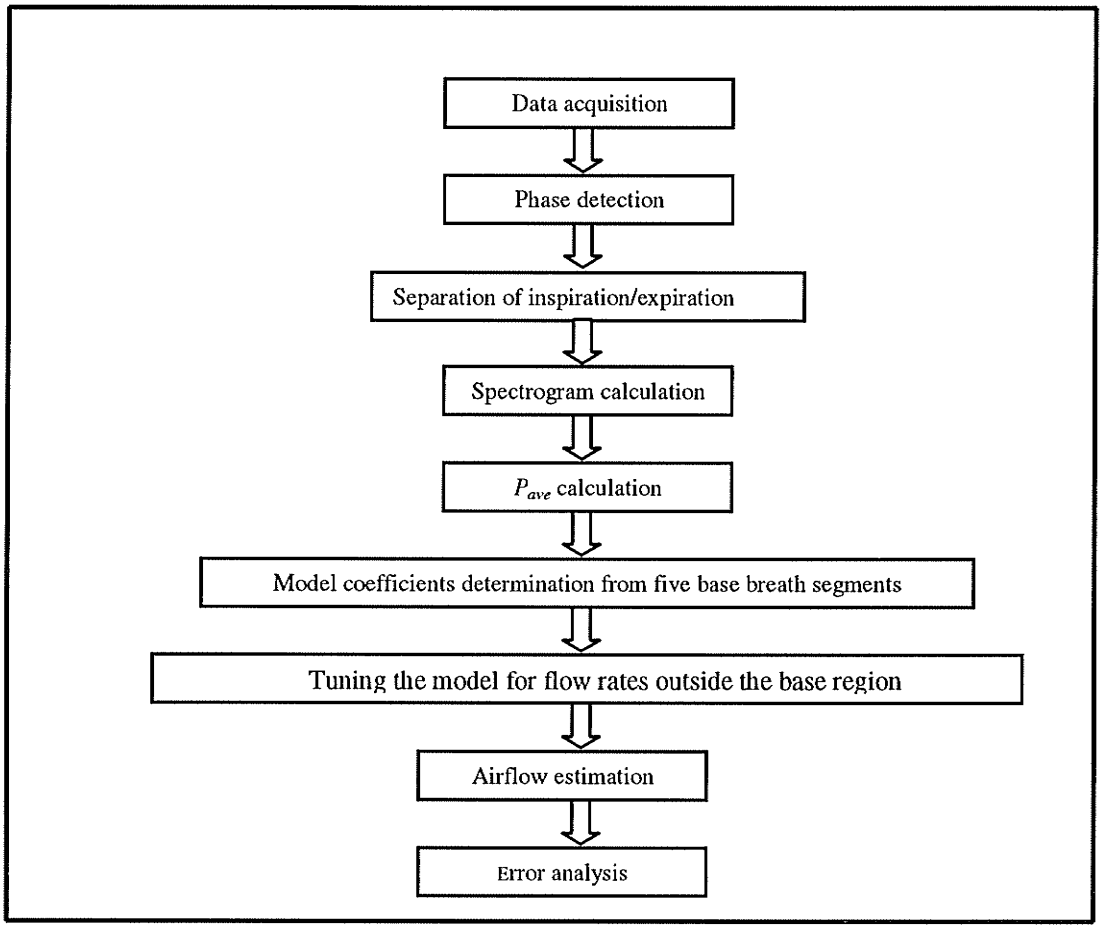

Figure 3.5. Summary for airflow estimation using tracheal sound average power.

X. Breath Onsets Detection

The same tracheal and airflow signals (acquired from section I of this chapter) were used for breath onsets detection. Figure 3.6 shows a typical sample of respiratory sound and its corresponded airflow

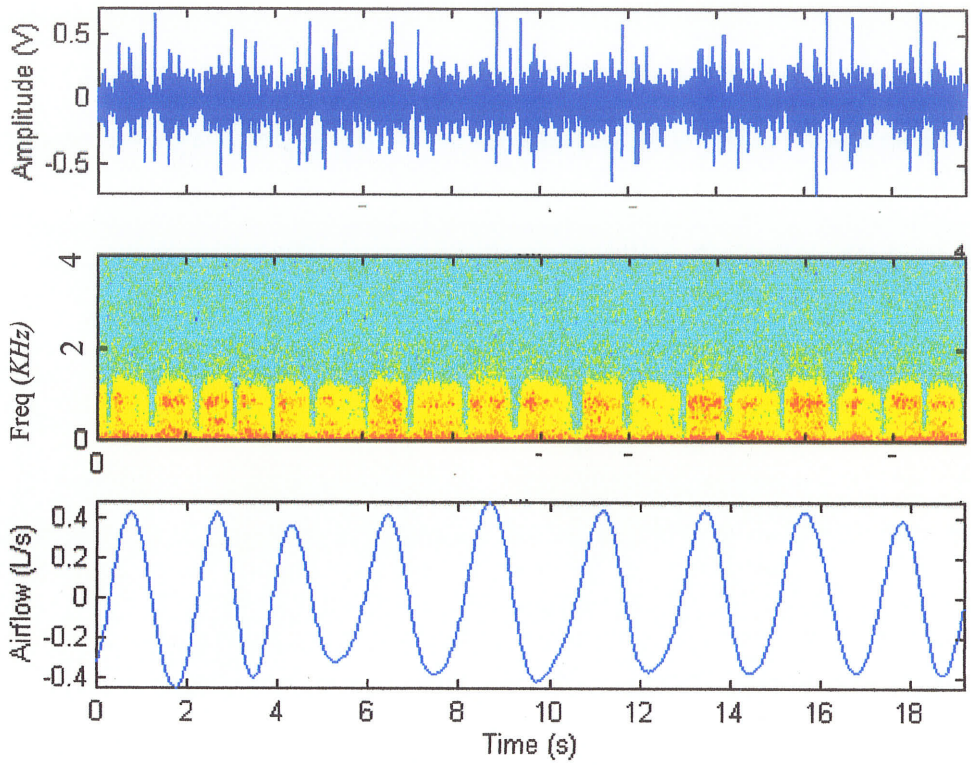

Figure 3.6. A typical tracheal breath sound signal with its associated spectrogram and airflow signal.

One definition defines chaos as a trajectory (signal progression) that is exponentially unstable and neither periodic nor asymptotically periodic. In other words, the function moves around seemingly randomly without ever settling into a fixed pattern. A recorded time series signal, representing chaotic or non-chaotic process can be

analyzed directly by examining the spread of the increments in the signal amplitude, i.e., variance, σ^2. Variance fractal dimension is defined as [Kinsner, 1995]:

$$D_\sigma = D_E - 1 + H , \qquad (3.4)$$

where D_E is the embedding dimension, which is the dimension of the embedding space (i.e., for a curve $D_E = 1$, a plane $D_E = 2$, and for space $D_E = 3$) and ,

$$H = \lim_{\Delta t \to 0} \frac{\log \mathrm{var}(\Delta S)_{\Delta t}}{2 \log(\Delta t)} , \qquad (3.5)$$

where S is the sound data samples and therefore ΔS is the variation of tracheal sound signal between two points as defined below:

$$\Delta t = | t_2 - t_1 |,$$

$$(\Delta S)_{\Delta t} = S(t_2) - S(t_1).$$

Figure 3.7 and 3.8 show $(\Delta S)_{\Delta t}$ and Δt graphically.

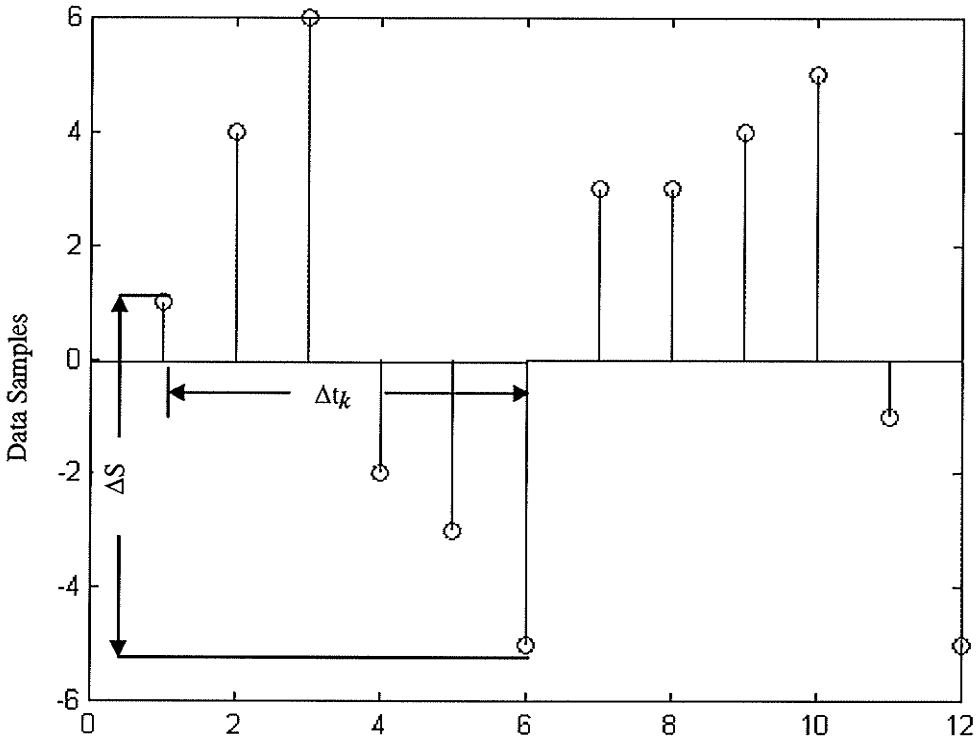

Figure 3.7. Illustrating $(\Delta S)_{\Delta t}$

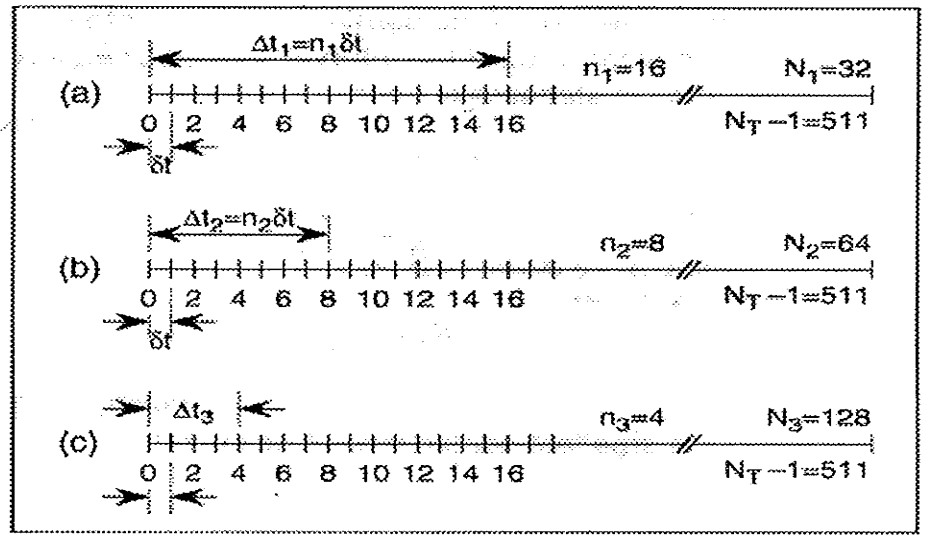

Figure 3.8. Illustrating the measurement scale Δt_k for D_σ calculation. For dyadic measurement scale $\Delta t_k = 2,4,8,16,32, \ldots$

To detect breath onsets, D_σ was calculated using N_T=128 points (12.5*ms*) with 50% overlap between the adjacent segments. Then, a running window with approximately half breath size (0.7 *s*) was used to detect all the peaks in D_σ.

CHAPTER 4 - RESULTS

I. Selecting the Base Region

Using Equation 3.3 with coefficients derived from different bases, the error of airflow estimation was calculated (Equation 3.2) and averaged between subjects. As can be seen in Figure 4.1, medium flow rate resulted in the lowest error. Therefore, medium flow rate was selected as the base region for deriving the model coefficients.

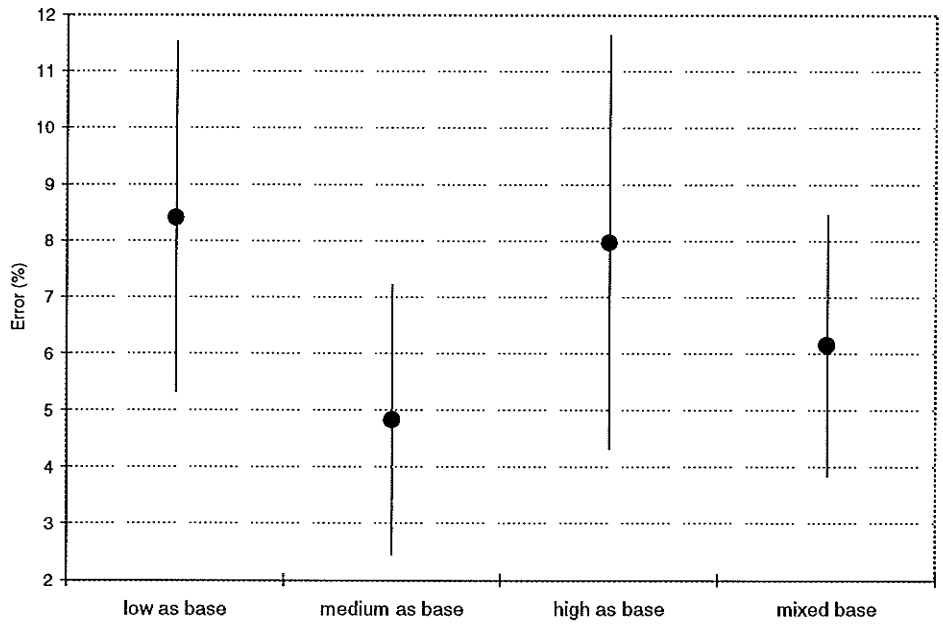

Figure 4.1. Comparison of airflow estimation error ($\mu \pm SE$) using different bases, considering only inspiration phases for each subject. Mixed base was investigated as a reference.

II. Optimizing Target Airflow Estimation

Using Equation 3.3 together with coefficients derived from medium flow rate, and by changing the lower limit of the fitting region, the error of airflow estimation was calculated (using Equation 3.2) and averaged between the subjects. The result showed slight differences in flow estimation error. However its mean and also standard deviation was minimum when the lower limit of 60% of flow was used (Figure 4.2). Therefore, P_{ave} and airflow from the upper 40% of the signal was used to derive model coefficients.

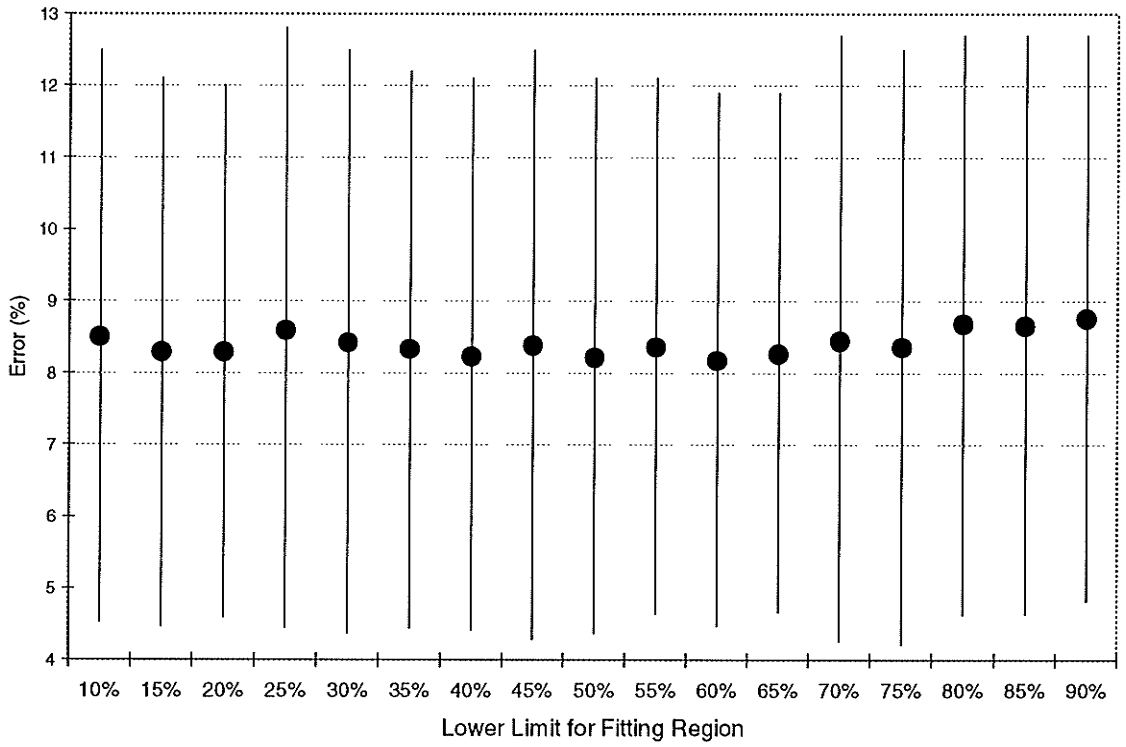

Figure 4.2. The averaged airflow estimation error ($\mu \pm SE$) using different lower limit of airflow when fitting P_{ave} to airflow for base segments.

III. Frequency Band to Calculate Average Power of Tracheal Sound

We also investigated the effect of using different frequency bands for P_{ave} calculation on airflow estimation. The results showed that the least error in airflow estimation from P_{ave} was calculated over the 150 – 450 *Hz* (Figure 4.3) band.

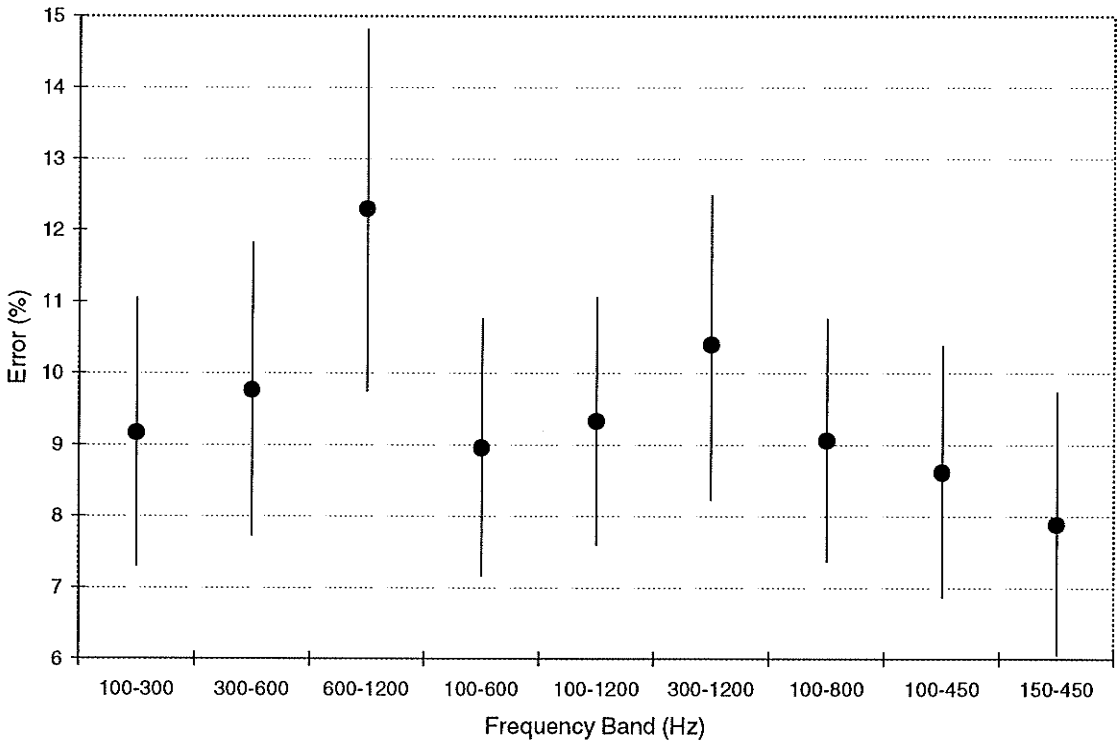

Figure 4.3. Averaged airflow estimation error (μ ± SE) for different frequency bands, considering only the inspiration phase.

IV. Result of Airflow Estimation

Choosing medium flow as a base region and calculating P_{ave} from 150 – 450 *Hz*, the entire airflow was estimated using Equation 3.3. Figure 4.4, 4.5 and 4.6 show a typical example of airflow estimation for both phases. The average error across ten subjects, was found to be 6.70 ± 1.79 % and 2.98 ± 0.78 % for inspiration and expiration respectively. Overall the error was found to be 4.84 ± 2.39 % across the ten subjects for both phases.

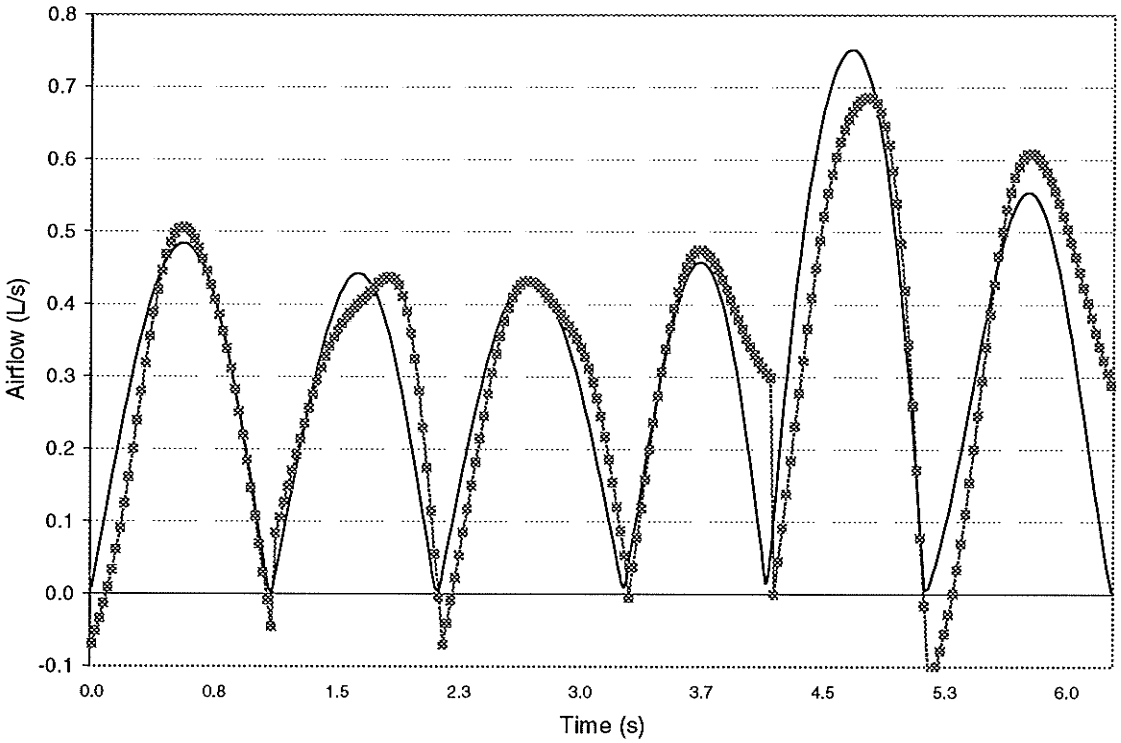

Figure 4.4. Actual flow (thin line) and estimated flow (thick line) for inspirations of a typical subject.

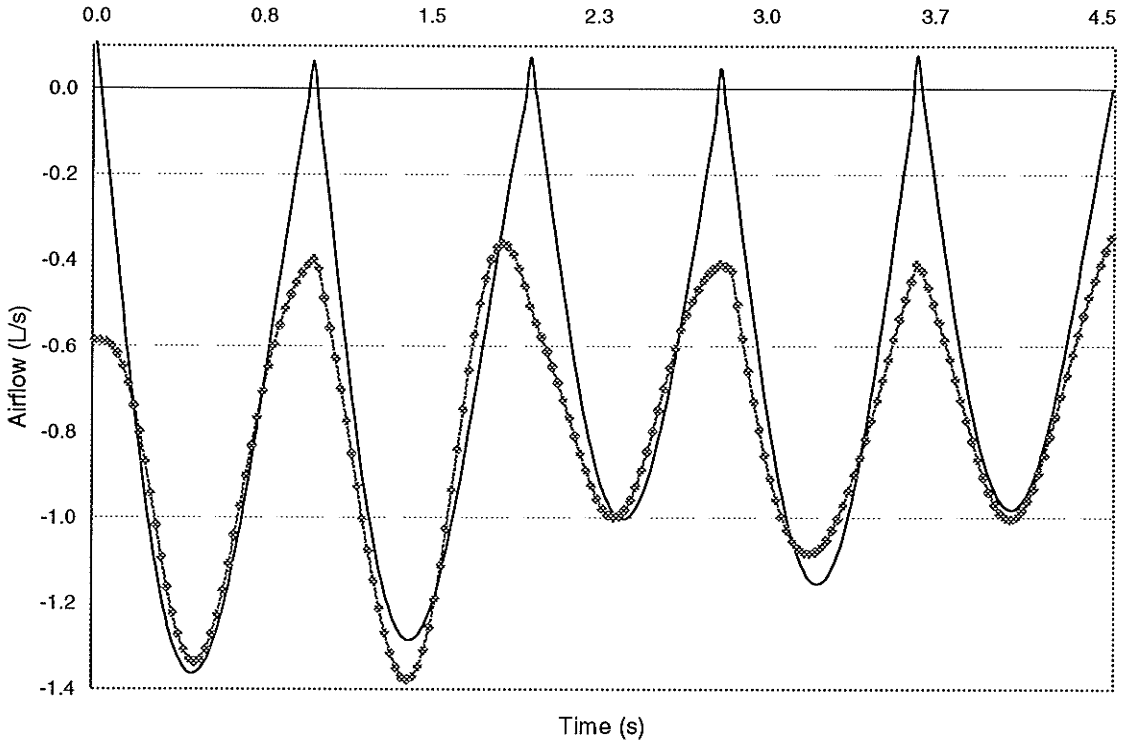

Figure 4.5. Actual recorded flow (thin line) and estimated flow (thick line) for expirations of a typical subject.

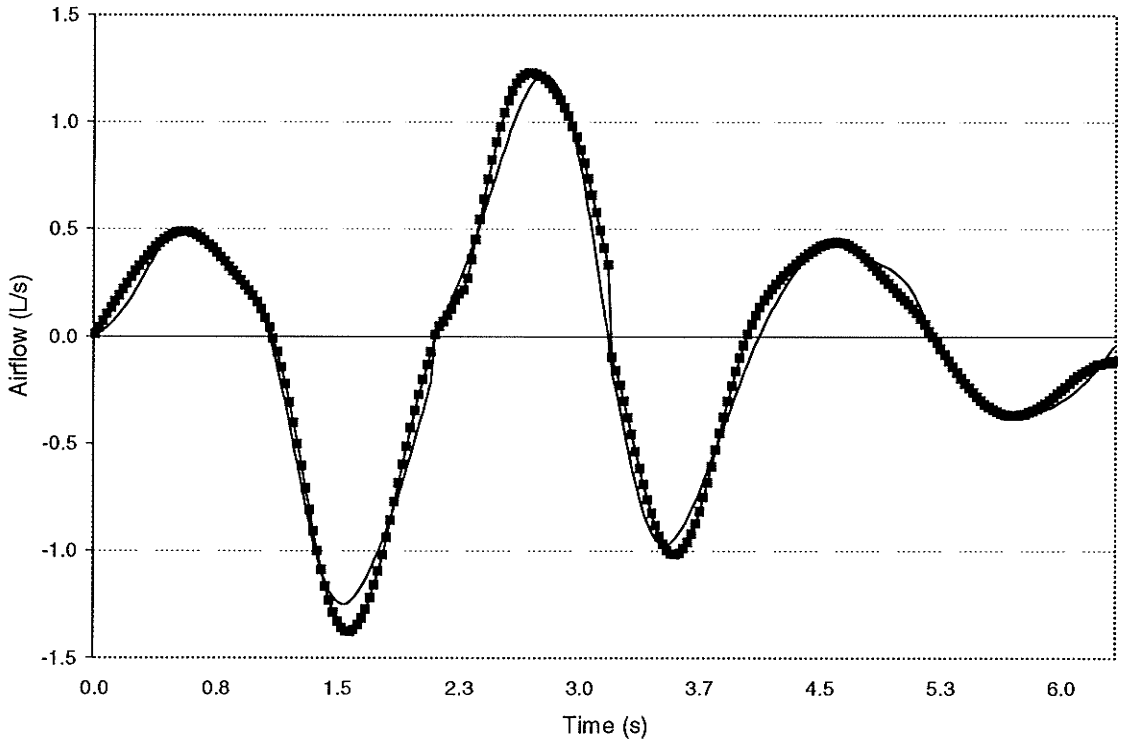

Figure 4.6. Actual flow (thin line) and estimated flow (thick line) for a typical subject.

V. Result for Breath Onsets Detection

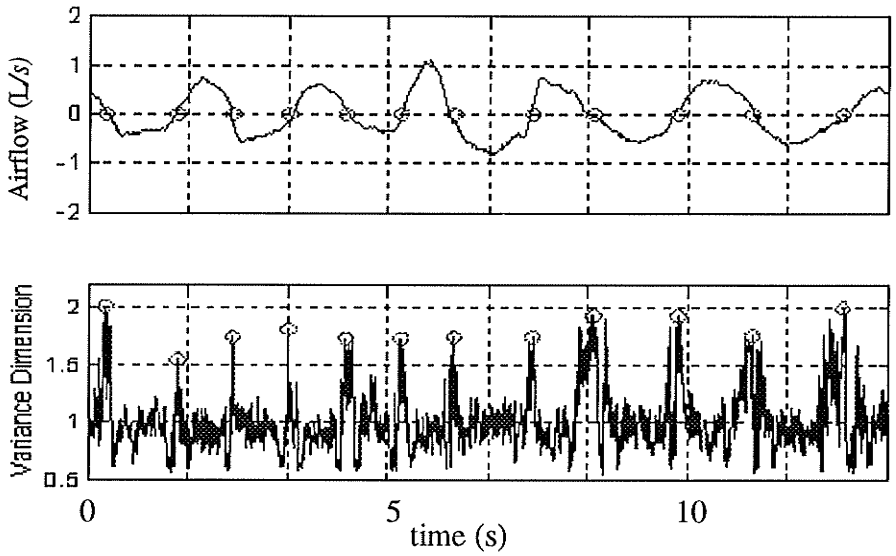

Figure 4.7. An actual airflow signal and the calculated variance fractal dimension. The circles are the detected locations of breath onsets in both plots.

Figure 4.7 shows the breath onsets detected from variance fractal dimension D_σ with the actual corresponded airflow. Comparing with the actual airflow, the result shows an average delay of 40±9 *ms* across nine subjects, which is slightly less than the delay presented in the previous study [Moussavi et al., 2000]. However, the standard deviation of the error in this method is much smaller than the precious one.

CHAPTER 5 - DISCUSSIONS & RECOMMENDATIONS

I. Discussion

Spectrogram is a 2D representation of a time-dependent signal spectrum. Darkness of the pattern is proportional to signal energy. As can be seen from Figure 5.1, the spectrogram intensity of tracheal respiratory sounds is directly related to the airflow rate, with its major components being concentrated below 2000 *Hz*.

The tracheal sounds and airflow signals in Figure 5.2 and 5.3 illustrate that P_{ave} is synchronized with the airflow cycles. As inspiration proceeds to peak intensity, P_{ave} follows the airflow accordingly with coinciding peaks. A similar time course is seen during expiration. Due to the synchronicity and close relation between the two variables (Figure 3.4), estimation of airflow using P_{ave} deems possible.

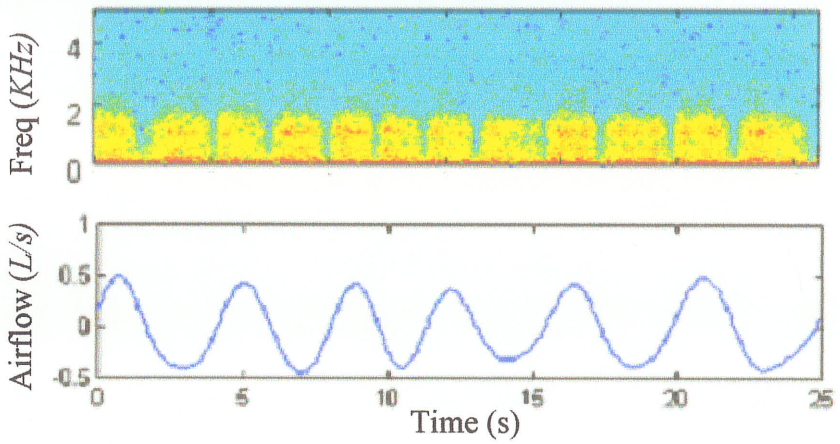

Figure 5.1. Spectrogram of tracheal sounds (top figure) and corresponding airflow (bottom figure).

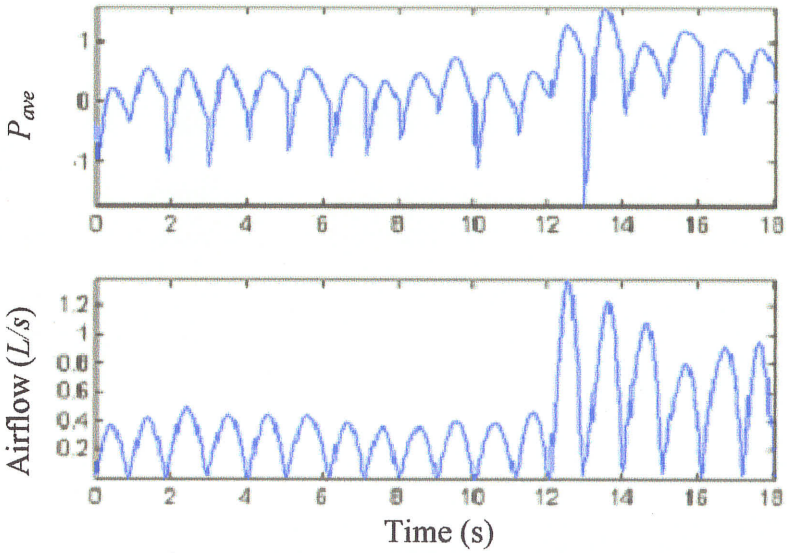

Figure 5.2. A typical P_{ave} with its corresponded airflow inspirations only.

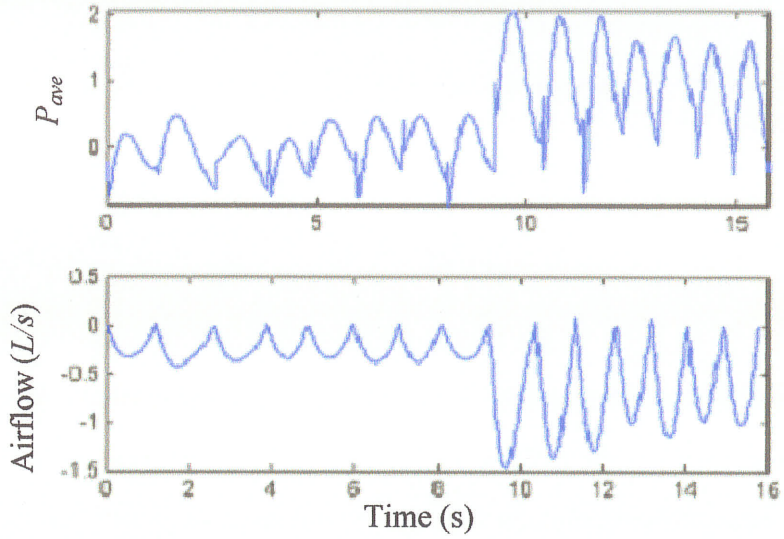

Figure 5.3. A typical P_{ave} with its corresponded airflow expirations only.

Tracheal sounds have been found to be a broad spectrum signal, higher in intensity compared to lung sounds, covering a frequency range from less than 100 *Hz* to more than 1500 *Hz*, wih a sharp attenuation (<-3*dB*, as shown in Figure 5.4) in energy above a cut-off frequency of approximately 800 *Hz* [Gavriely et al., 1981]. At high frequencies (>1500 *Hz*), white noise becomes prominent due to the diminishing tracheal sounds components. Therefore, we did not include frequencies components greater than 1500 *Hz* when calculating P_{ave}. Our result showed that the best frequency band to obtain P_{ave} was within 150-450 *Hz* (Figure 4.3) because it gave the lowest airflow estimation error.

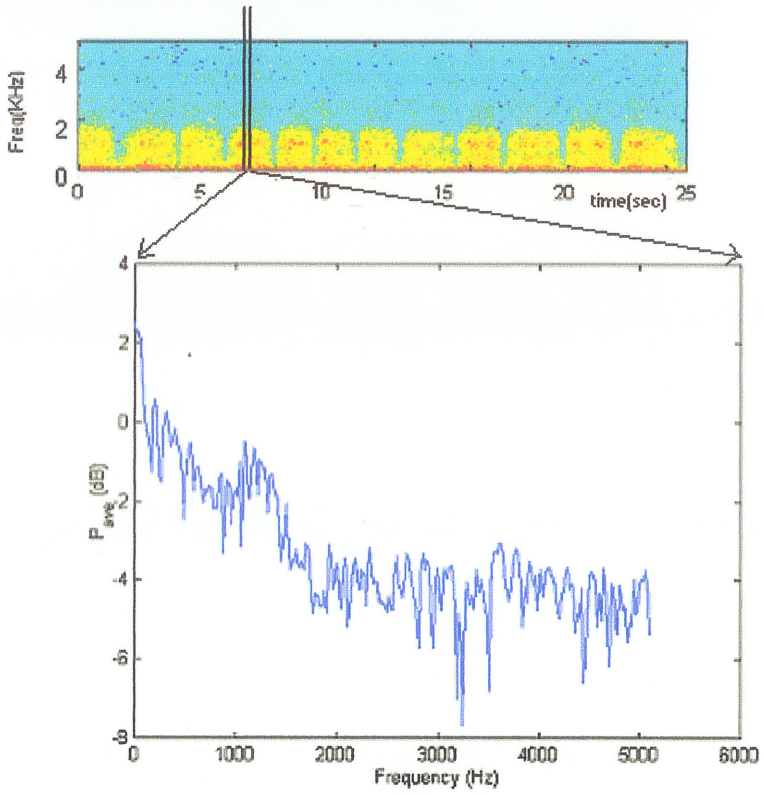

Figure 5.4. Tracheal sound spectrum (top figure) and the spectrum of one segment (bottom figure).

Although most of the components of tracheal sounds fall between 0 *Hz* – 1500 *Hz* for all subjects, each subject's signal had a considerably different shape of spectrum within this frequency band. This is in agreement with Pasterkamp's paper [Pasterkamp et al., 1997], that stated peaks and troughs of breath sound spectrum are related to airway conduit dimensions. Other researchers [Olson et. al., 1984] stated that recording tracheal sound at different sites (Upper or mid tracheal airway) will lead to different shape of tracheal sound and this is due to the different mechanism in breath sound generation. In other words, the spectral shape of tracheal sounds is highly variable between subjects but quite reproducible for the same person if recording was performed at a consitent site.

Therefore, in this study each subject had his/her own unique and special parameters for estimating airflow from $P_{ave,}$ and model parameters were derived separately for each subject's tracheal sound.

Given that the respiratory phases (inspiration/expiration) and their onsets can be determined acoustically [Moussavi et al., 2000], if the peak target flow region can be estimated accurately, this would ensure reconstruction of the entire airflow since the airflow between the phase transition (onsets) and peak target region is quite deterministic. To achieve this purpose, two strategies were employed. Firstly, we chose an optimum value of lower limit for fitting region to emphasize the peak target flow. This means that the modelexpressed in Equation (3.3) would follow the peak target flow region accurately, but looses its accuracy in the lower flow region, which is less important for the reason given above. Figure 4.2 summarized this trade-off and concluded that fitting the upper forty percent of airflow (lower limit equivalent to 60% of F_{max}) to P_{ave} was the optimum parameter. Secondly, the error Equation (3.2) was defined in such a way that emphasizes on the upper 15% of airflow such that the selection of the base region and frequency band for P_{ave} would optimize the peak target flow estimation. In a real scenario, physicians and researchers are mostly concerned of the peak target flow and its relationship with the amplitude and frequency spectrum of the respiratory sounds [Nishimaki et al., 1987; Shykoff et al.,1988].

The scaling factor in Equation (3.3) was added to the original Equation (3.1) to justify the estimated airflow for different target flows outside of the base segment. It was

derived from the ratio of instantaneous power to the average peak power of base segments. For example, when high flows are being estimated, its associated instantaneous power would be greater than the average peak power of base segments (medium flow). Thus, the scaling factor would adjust the underestimation (Figure 3.5) by multiplying it by a value greater than 1. The reverse happens when low flows are being estimated. The scaling factor was chosen in a way that it remains 1 for the airflow at the level of base segments, where the coefficients of the model were derived and optimized.

Artifacts during recording may create inconsistencies between P_{ave} and airflow. For example, the boxed region in Figure 5.5 shows an inconsistency between P_{ave} and actual flow as a result of an artifact. Therefore, it is suggested a program to detect the artifacts and remove them from the tracheal sound before airflow estimation. In this study however, the bad segments (segment with artifacts) were removed manually.

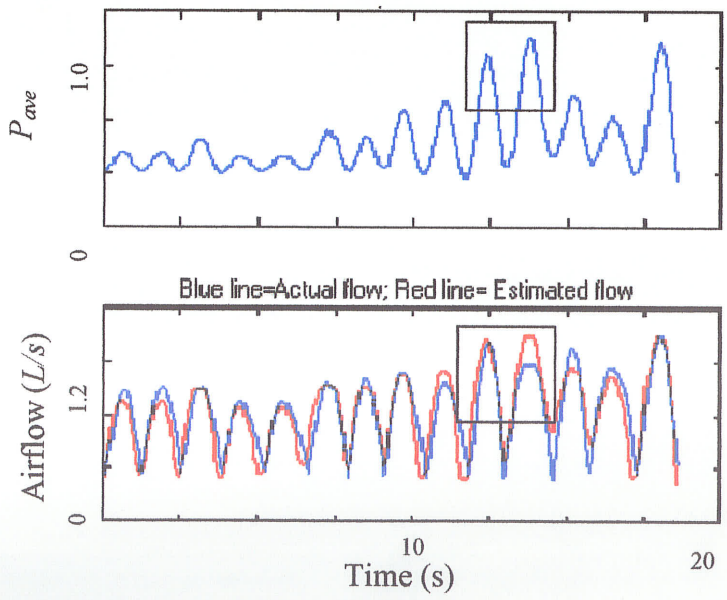

Figure 5.5. Boxed region shows inconsistency between P_{ave} and actual flow. It causes error in estimated flow (red line).

In the earlier part of this chapter, it was mentioned that different subjects' signals had different spectral characteristics. Thus, each signal had its own unique coefficients. This has been consistently observed in the findings of this research (Figure 5.6 and 5.7). However, the common element between the subjects was that P_{ave} and flow follow the general pattern (exponential relationship) and this pattern was mostly pronounced in a particular frequency band (100-450 Hz).

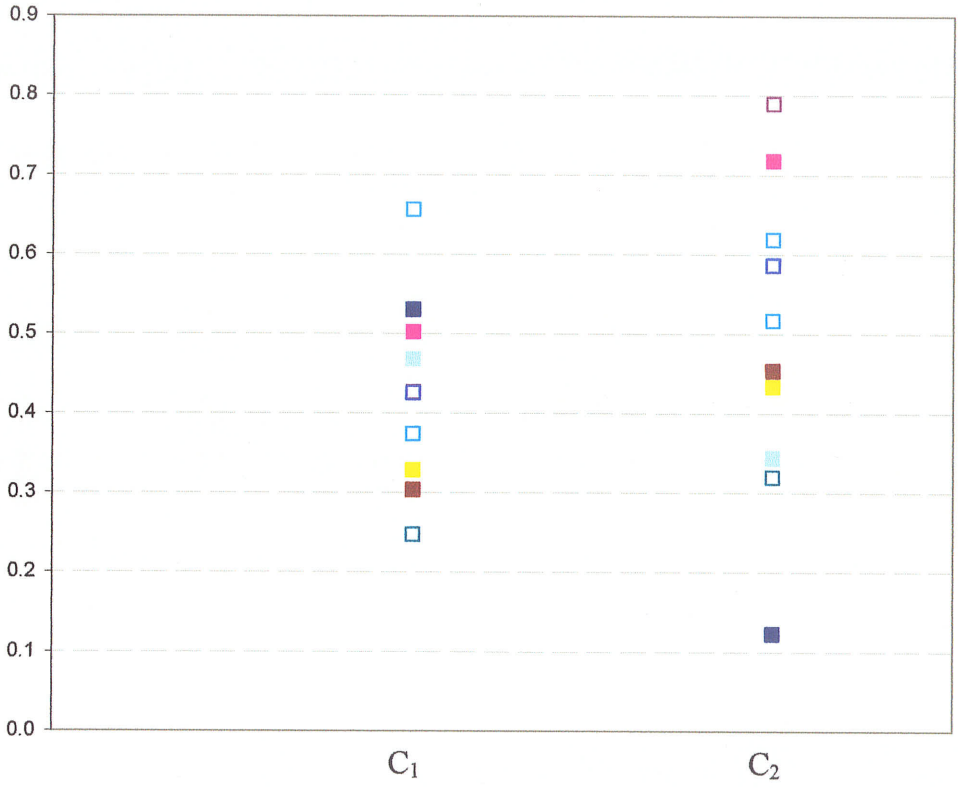

Figure 5.6. C_1 and C_2 coefficients for the ten subjects for Inspiration.

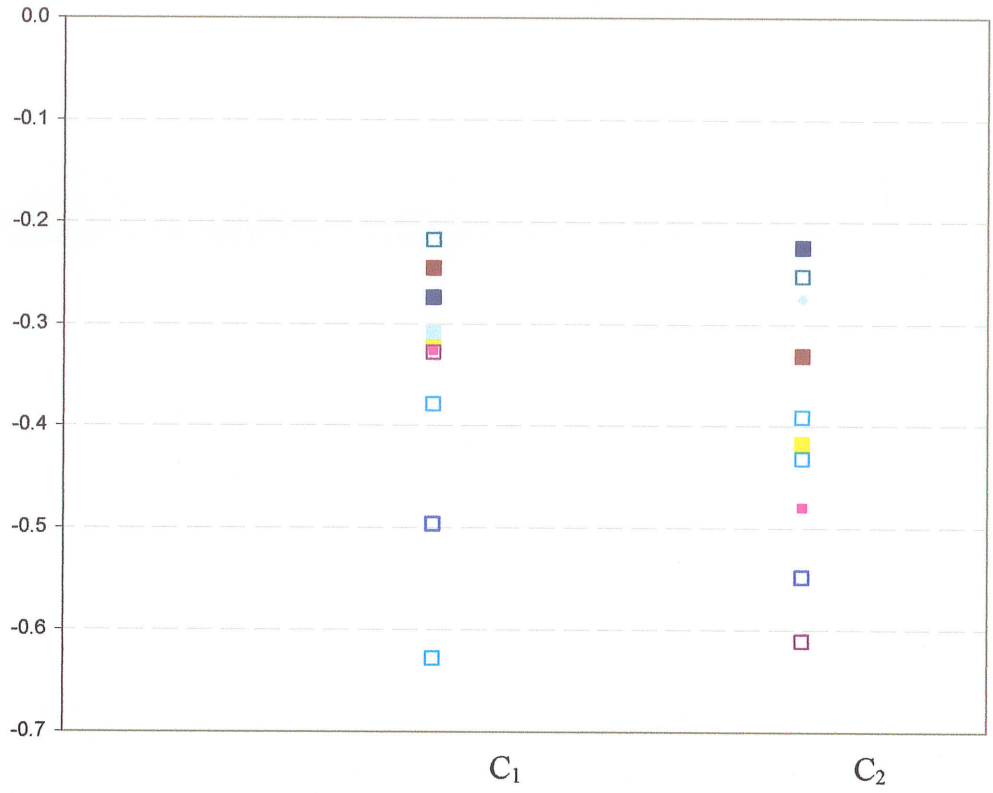

Figure 5.7. C_1 and C_2 coefficients for the ten subjects for expiration.

It is also obvious in the two figures above that the model coeffcients for the inspiratory and expiratory phases are different within the same subject's signal. For this reason, it is important to separately analyze inspiratory and expiratory sounds.

The only research that actually estimated airflow from the tracheal sounds was the work by Soufflet and his co-worker [Soufflet et al., 1990]. They evaluated airflow from tracheal sounds using eight methods, using reference curves in four of them and using clustering analysis in the other four. Their results indicated a substancial variability between subjects, as reflected in the shape of the reference curves. This is in agreement

with our findings as it is shown in Figures 5.6 and 5.7. For the implementation of the reference curve method, they used four different parameters to derive the reference curve: 1) mean amplitude of tracheal sounds, 2) mean aplitude of tracheal sound spectrum, 3) mean frequency of tracheal spectrum and 4) product of mean amplitude and mean frequency. These methods gave a mean uncertainty of 14% when used to estimate unknown airflow. The high error could possibly be caused by the use of a flow transducer during signal acquisition. As noted earlier [Mussell et al., 1990], flow transducers significantly alter the spectral parameters of tracheal sounds, specifically frequency of maximum amplitude (FMA), mean frequency of the spectra (MFA) and maximum frequency (MF). In Mussell's paper, tracheal sounds measured together with a flow transducer showed additional extra spectra peaks and harmonics, which were not seen when the flow transducer was not used. This is not the case in this study because these spectral peaks and harmonics (if any) were cancelled off during the subtraction of background noise. Apart from that, another difficulty faced by the reference curve method cencerns the evaluation of very small flows since the reference curves are almost parallel to the flow axis and are highy sensitive to noise. Therefore, using a mathematical model equation to estimate airflow is by far a better methodology.

Gavriely and co-workers [Gavriely et al., 1996] suggested the power relationship model but did not use the model to estimate unknown airflow. In this study, our decision to choose an exponential model instead of the power model was supported by the evaluation of the correlation coefficients of the best fit linear regression lines of the two types of relationship.

Several points arose from this study on the relationship between tracheal sounds and airflow and using these sounds to estimate airflow. We were able to investigate: 1) the best quatitative relationship equation between P_{ave} and airflow, 2) the best base region for deriving model coefficients, 3) the best frequency band to compute P_{ave}, 4) the best lower limit for fitting region. The main achievement in this study was that using the exponential model suggested, we were able to derive model coefficients and use them to estimate unknown airflow in an automated fashion. However, there are a few drawbacks. The program is very sensitive toward the tracheal and airflow signals at the base region since the model coefficients are derived from them. If the two variables (P_{ave} and airflow) are not consistent in their relationship, inccurate model coefficients would be computed. Hence, it leads to high error during airflow estimation. In our data, preprocessing was needed to yield consistent signals.

The breath onsets were also detected acoustically in this study. The only base for comparison is the recent research, in which the tracheal average P_{ave} was used to detect breath onsets and their results showed an average delay of 42±35 *ms* [Moussavi et al., 2000]. In this study, we postulated that during the transition of breath phases, the sound signal has a temporal chaotic feature due to the momentum of airflow as it changes its direction. Hence, this leads to a chaotic process, which can be detected by its signal complexity using variance fractal dimension D_σ. As can be seen in 4.7, variance fractal dimension approaches a value of two, indicating the signal during transition of phases has a complexity between a line and a plane. It can not be a pure line because all data points do not lie in a straight line; it can not be a plane as well since the area for one-

dimensional signal is zero. This important characteristic of non-integer fractal dimension has been used extensively in describing and classifying speech phonemes [Fekkai et al., 2000].

The advantage of variance fractal dimension D_σ is that it does not compromise between frequency and time resolution, while the accuracy of breath onsets detection by the average power method depends on the windows size to segment data and the window size option is limited by the trade-off between the time and frequency resolution. D_σ, however, concerns solely with time resolution N_T. By changing the size of N_T, the magnitude of D_σ also changes. An Optimum N_T interval is obtained when D_σ shows prominent peaks.

Another important aspect of variance fractal dimension D_σ is that it can be calculated directly in the time domain. It can be programmed to have a real-time procedure to calculate D_σ while tracheal sound signals are being received. Overall, the result of breath onsets detection using variance fractal dimension is encouraging. Further experiments have to be carried out to examine whether variance fractal dimension is also useful in determination of respiratory phases from the chest sound signals.

II. Future Research Recommendation

In spite of different models investigated (linear, power and exponential relationship models), the exponential model gave the best result with an appropriate scaling factor. This result confirmed that tracheal sounds allowed airflow estimation with an error of less than 5%. If the error deemed to be within an acceptable range (<10% for target airflow estimation) across larger amount of subjects and patients, then the proposed method will have the potential of replacing the conventional methods of measuring airflow which encounter difficulty during feeding assessment. Furthermore, since subjects may also swallow during respiratory-related assessment, the current technique of airflow estimation must be used with a swallowing detection algorithm, which requires additional signal processing to have a reliable and accurate detection routine, so that it would not lead to erroneous airflow estimation.

Apart from the above recommendations, there is room for improvement in the signal acquisition of tracheal sounds and airflow signals. Future work should assure a higher quality tracheal sound and airflow signals with low noise and artifacts. Any inconsistencies due to hardware or software problems should be minimized. Alternatively, the program could be improved by incorporating the detection of artifact and inconsitencies automatically.

In addition to current research on tracheal sound, continuation of this study to the relationship of lung sounds and airflow may also contribute to a broader understanding of

REFERENCES

1. Abella M., Formolo J. and Penny DG., "Comparison Acoustic Properties of Six Popular Stethoscopes", *J. Acous. Soc. Am.,* 91: 2224 – 2228, 1992.
2. Beckerman R. and Wegamm M., "A Comparison of Tracheal Breath Sounds, Airflow, and Impedance Pneumography in the Detection of Childhood Apnea", *Sleep*, 8: 342-346, 1985.
3. Bullar JF., "Experiment to Determine the Origin of Respiratory Sounds", *Proc. R. Soc. Med.,* 37:411, 1884.
4. Charbonneau G., Sudraud M., and Soufflet G., "A Method to Evaluate Flow Rate From Breath Sounds), *Bull. Eur. Physiopathol. Respir.,* 23:265-270, 1987.
5. Charbonneau G., Ademovic E., Cheetham B.M.G., Malmberg L.P., Vanderschoot J. and Sovijavi A.R.A., " Basic Techniques for Respiratory Sound Analysis", *Eur. Respir. Rev.,* 2000; 10: 77, 625-635, 2000.
6. Cheetham B.M.G., Charbonneau G., Giordano A., Helisto P., Vanderschoot J., "Digitization of Data for Respiratory Sound Recordings", *Eur. Respir. Rev.,* 10:77, 621-624, 2000.
7. Cummiskey J., William T., Krumpe P. and Guileminault C., "The Detection and Quantification of Sleep Apnea by Tracheal Sound Recording", *Am. Rev. Respir. Dis.*, 126:221-224 1982.

8. Earis J.E. and Cheetham B.M.G., "Current Methods Used For Computerized respiratory Sound Analysis", *Eur. Respir. Rev.,* 10:77, 586-590, 2000.

9. Earis J.E., Cheetham B.M.G., "Future Perspectives for Respiratory Sound Research", *Eur. Respir. Rev.,* 10:77, 641-646, 2000.

10. Fahr G., "The Acoustics of Bronchial Breath Sounds", *Arch. Intern. Med.,* 39:286, 1927.

11. Faloutsos C. and Kamel I., "Beyond Uniformity and Independence: Analysis of R-Trees Using the Concept of Fractal Dimension", *Proc. ACM SIGACT-SIGMOD-SIGART PODS*, Minneapolis, MN, May 24-26, pp. 4-13, 1994.

12. Faloutsos C. and Gaede V., "Analysis of Z-Ordering Method Using the Hausdorff Fractal Dimension", *Conf. On Very Large Databases* (VLDB), Bombay, India, Sept., 1996.

13. Fekkai S., Al-Akaidi M. and Blackledge J.M., "Fractal Speech Processing" *IMA Conf. On Fractal Geometry: Mathematical Techniques, Algorithms and Applications*, Sept. 20, 2000.

14. Forgacs P., "Lung Sounds", London, England: Bailliere Tindall, 1978.

15. Forgacs P., "The Functional Basis of Pulmonary Sounds", *Chest* 73: 399-405, 1978.

16. Gasquet C. and Witomski P., "Analyse De Fourier et Application", Paris, *Masson*, 1990.

17. Gavriely N. and Cugell D.W., "Airflow Effect on Amplitude and Spectral Content on Normal Breath Sounds", *J. Appl. Physiol.,* 80:5-13, 1996.

18. Gavriely N., Palti Y. and Alroy G., "Spectral Characteristics of normal breath sounds", *J. Appl. Physiol.,* 50:307, 1981.

19. Hudson D., Conn R., Matsubara Y. and Pribble Y., "Rales – Diagnostic Uselessness of Qualititive Adjectives", *Am. Rev. Respir. Dis.,* 113:187, 1978.

20. Kinsner W., "A Unified Approach to Morphological Entropy, Spectral and Variance Fractal Dimension", *10th Intern. Conf. On Mathematical and Computer Modeling Record, ICMCM*, Boston, MA., July 5-8, 1995.

21. Kinsner W. and Grieder W., "Fractal Amplification of Signal Feature Using Variance Fractal Dimension", *10th Intern. Conf. On Mathematical and Computer Modeling Record, ICMCM*, Boston, MA., July 5-8, 1995.

22. Kraman S.S, Pasterkamp H., Kompis M., Takase M. and Wodicka G., "Effect of Breathing Pathways on Tracheal Sound Spectral Features", *Respir. Physiol.,* 111: 295-300, 1998.

23. Kraman S.S., "The Relationship Between Airflow and Lung Sound Amplitude in Normal Subjects", *Chest*, 86:2: August, 1984.

24. Kraman S.S., "Effect of Lung Volume and Airflow on The Frequency Spectrum of Vesicular Lung Sounds", *Respir. Physio.* 66, 1-9, 1986.

25. Leannec R.T.H., "a Treatise on the Disease of the Chest and Mediate Auscultation" (in French) 1819, translated in *J. Forbes. New York*: Samuel Wood, 1935.

26. Leblanc P., Machlem P.T. and Ross W.R.D., "Breath Sounds and Distribution of Pulmonary Ventilation", *Am. Rev. Respir.* Dis., 102: 10-16, 1970.

27. Lessard C.S. and Wong W.C, "Correlation of Constant Flow Rate with Frequency Spectrum of Respiratory Sounds When Measured at the Tracheal", *Trans. on Biomed. Eng.*, Vol. BME-33, No. 4 April 1986.

28. Moussavi Z., Leopando M.T., Pasterkamp H. and Rempel G., "Computerized Acoustical Respiratory Phase Detection Without Airflow Meansurement", *Med. and Biol. Eng. and Comput.,* 38 (2):198:203, March 2000.

29. Murphy R.L., Holford S.K. and Knowles W.C., "Visual Lung Sound Characterization by Time-Expanded Waveform Analysis", *N. Engl. J. Med.,* 296:968-971,1977.

30. Mussell M.J., Nakazono Y. and Miyamoto Y., "Effect of Airflow and flow transducer on Tracheal Sounds", *Med. & Biol. Eng. & Comput.*, 28, 550-554, 1990.

31. Mussell M.J., Nakazono Y., Miyamoto Y., Okabe S. and Takashima T., "Distinguishing Normal And Abnormal Tracheal Breathing Sounds By Principle Component Analysis", *Jpn. J. Physiol.*, 40 713-721, 1990.

32. Mussell M.J. and Miyamoto Y., "Comparison of Normal Respiratory Sounds Recorded from the Chest and Tracheal at Various Respiratory Airflow Levels", *Front. Med. Biol. Eng.*, Vol. 4, No. 2, pp. 73-85 1992.

33. Olson D.E., Bogyi M., Schwartz D.B. and Hammersley J.R., "Relationship of Tracheal Sounds to Airflow", *Am. Rev. Respir.*, Dis. 129:A256, 1984.

34. Olson D.E. and Hammersley J.R., " Mechanism of Lung Sound Generation", *Semin. Respir. Med.* 6:171-179, 1985.

35. Pasterkamp H., "Respiratory Sounds", *Am. J. Respir. Crit. Care Med.*, Vol. 156. pp. 974-987, 1997.

36. PasterKamp H., Kraman S.S., DeFrain P.D. and Wodicka G.R., "Measurement of Respiratory Acoustical Signals—Comparison of Sensors", *Chest* 104:1518-1525 1993.

37. Piirilla P., Sovijarvi A.R.A., Earis J.E., Rossi M., Dalmasso F., Stoneman S.A.T. and Vanderschoot J., "Reporting Results of Respiratory Sound Analysis", *Eur. Respir. Rev.,* 10:77, 636-640, 2000.

38. Plate F., Kessler H., Sun X.Q., Cheetham B.M.G. and Earis J.E., "Inverse Filtering Applied to Upper Airway Sounds". *Technol Healthcare* 6: 23-32, 1998.

39. Ploysongsang Y., Pare J.A.P., Macklem P.T., "Correlation of Regional Breath Sound with Regional Ventilation In Emphysema", *Am. Rev. Respir.* Dis., 126:526-529, 1982.

40. Priestley M.B., "Spectral Analysis and Time Series", New York, Academic Press, 1981.

41. Rossi M., Sovijarvi A.R.A., Piirila P., Vannuccini L., Dalmasso F. and Vanderschoot J.. "Environment and Subject Conditions and Breathing Manoeuvres for Respiratory Sound Recordings", *Eur. Respir. Rev.,* 10:77, 611-615, 2000.

42. Sanchez I. And Pasterkamp H., "Tracheal Sound Signal Depends on Body Weight", *Am. Rev. Respir.* Dis., 148: 1083-1087, 1993.

43. Shykoff B.E., Ploysongsang Y. and Chang H.K., "Airflow and normal lung sounds", *Am. Rev. Respir.* Dis., 137: 872-876, 1988.

44. Soufflet G., Charbonneau G., Polit M., Attal P., Denjean A., Escourrou P. and Gaultier C., "Interaction Between Tracheal Sound and Flow rate: A Comparison of Some Different Flow Evaluations from Lung Sounds", *IEEE Tran. on Biomed. Eng.,* Vol. 37, No. 4, April 1990.

45. Sovijarvi A.R.A., Dalmasso F., Vanderschoot J., Malmberg L.P., Righini G., Stoneman S.A.T., "Definition of Terms for Applications of Respiratory Sounds", *Eur. Respir. Rev.,* 10:77, 597-610, 2000.

46. Sovijarvi A.R.A., Vanderschoot J., Malmberg L.P., Charbonneau G., Dalmasso F., Sacco C., Rossi M. and Earis J.E., " Characteristics of Breath Sounds and Adventitious Respiratory Sounds", *Eur. Respir. Rev.,* 10:77, 591-596, 2000.

47. Sovijarvi A.R.A., Vanderschoot J. and Earis J.E., "Standardization of Computer Respiratory Sound Analysis", *Eur. Respir. Rev.,* 10:77, 585, 2000.

48. Tarrant S.C., Ellis R.E., Flack F.C., Selley W.G., "Comparative Review of Techniques for Recording Respiratory Event at rest and During Deglutition", *Dysphagia* 12, 24-38, 1997.

49. Traina C., Traina A., Wu L., and Faloutsos C., "Fast Features Selection Using the Fractal Dimension", *XV Brasilian Symp. On Databases* (*SBBD*), Paraiba, Brazil, Oct., 2000.

50. Vannuccini L., Earis J.E. and Helisto P., Cheetham B.M.G., Rossi M., Sovijarvi A.R.A., Vanderschoot J., "Capturing and Preprocessing of Respiratory Sounds", Eur. Respir. Rev., 10:77, 616-620, 2000.

51. Wodicka G., Stevens K.N., Golub H.L and Shannon D.C, "Spectral Characteristics of Sound Transmission in the Human Respiratory System", *IEEE Tran. on Biomed. Eng.*, Vol. 37. No. 12, Dec 1990.

52. Wodicka G., Aguirre A., DeFrain P.D., Shannon D.C., "Phase Delay of Pulmonary Acoustic Transmission from Tracheal to Chest Wall", *IEEE Tran. On Biomed. Eng.*, Vol. 39. No. 10, Oct. 1992.

53. Yap Y.L.and Moussavi Z., "Acoustical Airflow Estimation from Tracheal Sound Power", *Proc. IEEE CCECE,* 2002.

54. Yonemaru M., Kikuchi K., Mori M., Kawai A., Abe T., Kawashiro T., Ishihara T., Yokoyama T., "Detection of Tracheal Stenosis by Frequency Analysis of Tracheal Sounds", *The American Physio. Soc.* 0161-7567, 1993.